

DOI: 10.1002/cmdc.200900283

Activators of P-glycoprotein: Structure–Activity Relationships and Investigation of their Mode of Action

Katja Sterz, Lars Möllmann, Anna Jacobs, Dieter Baumert, and Michael Wiese^{*[a]}

P-glycoprotein (P-gp), a 170 kDa plasma membrane protein, is one of the most relevant ABC transporters involved in the development of multidrug resistance (MDR). Understanding its mechanism of transport as well as its interactions with various substrates are basic requirements for the development of adequate therapeutic approaches to overcome this kind of resistance against a broad spectrum of structurally unrelated cytostatic drugs. P-gp modulators (activators) that exert various effects on the intracellular accumulation of distinct P-gp substrates are useful tools for investigating the interactions between multiple drug binding sites of this transport protein. In this study, a series of 27 different imidazobenzothiazoles and imidazobenzimidazoles structurally related to the known P-gp

activators QB102 and QB11 was designed, and their modulating properties were investigated. Most of them were able to stimulate P-gp-mediated efflux of daunorubicin and rhodamine 123 in a concentration-dependent manner, but some compounds also displayed weak inhibitory effects. Additionally, P-gp-mediated efflux of vinblastine and colchicine was inhibited by several compounds. Therefore, we concluded that the novel compounds bind to the H site of P-gp and activate the efflux of specific substrates of the R site in a positive cooperative manner, whereas binding of H-type substrates is inhibited competitively. This hypothesis is confirmed by the observation that the modulators do not influence hydrolysis of ATP or its affinity toward P-gp.

Introduction

P-glycoprotein (P-gp, ABCB1) belongs to the family of ABC transporters and is widely distributed in various tissues. It provides a barrier function in the human body in such areas as the blood–brain barrier, liver, and placenta. Therefore, it plays an important role in protecting the body against a wide variety of xenobiotics and in the distribution and elimination of drugs.^[1,2] On the other hand, overexpression of P-gp in tumor cells contributes to the phenomenon of multidrug resistance (MDR), which is a major obstacle in the chemotherapy of lymphomas, leukemias, and many solid tumors. MDR cells become insensitive against a wide variety of structurally unrelated cytostatic drugs such as anthracyclines, *Vinca* alkaloids, and taxanes, leading to failure of chemotherapy. Additionally, many other compounds such as antiviral drugs, antibiotics, and fluorescent dyes like rhodamine and Hoechst derivatives are substrates transported by P-gp.^[3]

Although P-gp is one of the best-characterized ABC transporters, the mechanism of substrate transport and its coupling to ATP hydrolysis is not finally elucidated. In particular, concerning the number and location of possible drug binding sites, several theories have been published over the past few years, reporting up to seven putative binding sites located in the transmembrane (TM) domains of the protein.^[4–6] However, it is generally accepted that TM helices 5, 6, 11, and 12 are involved in substrate binding. One popular model was published by Shapiro and Ling suggesting two different functional binding sites that interact in a positive cooperative manner.^[4] Rhodamine 123 and anthracyclines are substrates of the so-called R site, whereas Hoechst derivatives and colchicine, among others, belong to the H-type of P-gp substrates. This two-site

hypothesis is one of the most convenient working models for explaining the mutual stimulation of P-gp-mediated transport by several substrates. There is also evidence for a third allosteric binding site, exhibiting a regulatory function, where, for example, progesterone binds.^[7]

In the past few years a broad spectrum of inhibitors has been developed in order to overcome P-gp-mediated MDR.^[8,9] Some of these compounds, effectively decreasing resistance of MDR cells *in vitro*, have even reached phase III clinical trials, but so far no satisfactory benefit of co-administering P-gp inhibitors with cytostatic drugs has been achieved.^[10,11] Furthermore, several substances such as flavonoids and some hydrophobic peptides, which are able to activate substrate transport by P-gp, have been described.^[12,13] Kondratov et al. identified several small molecules, first designed as inhibitors of the protein p53, with different effects on the cellular accumulation of distinct P-gp substrates.^[14] The most potent compounds QB102 (pifithrin- α cycl.) and QB11 (Figure 1) stimulated transport of anthracyclines and rhodamine 123, whereas efflux of *Vinca* alkaloids and Hoechst 33342 was inhibited. A particularly interesting aspect of this work^[14] is that the effect of the modulators seems to depend at least partially on the substrate binding site postulated by Shapiro and Ling.^[4] The investigation of this class of modulators may therefore contribute to a

[a] K. Sterz,⁺ L. Möllmann,⁺ A. Jacobs, D. Baumert, Prof. Dr. M. Wiese
Institute of Pharmacy, University of Bonn
An der Immenburg 4, 53121 Bonn (Germany)
Fax: (+49) 228 737929
E-mail: mwiese@uni-bonn.de

[*] These authors contributed equally to this work.

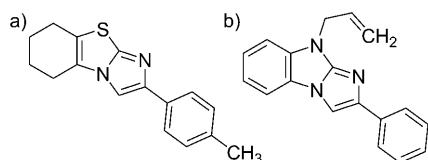


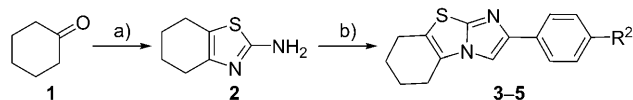
Figure 1. Structures of the published P-gp activators: a) QB102 and b) QB11, parent compounds of the analogues reported herein.

deeper understanding of the interactions between the different functional binding sites of P-gp.

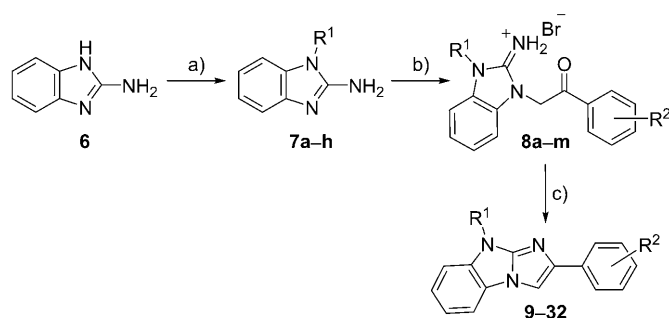
In this study a series of 27 imidazobenzimidazoles and imidazobenzothiazoles structurally related to QB102 (**3**) and QB11 were synthesized, and their influence on the cellular accumulation of rhodamine 123 (rho 123) and daunorubicin (DNR) was investigated in a flow-cytometry-based assay. The novel derivatives showed a similar behavior to that of the substances described by Kondratov et al.,^[14] and the most potent compounds yielded half-maximal activation in the high nanomolar concentration range. In a second step we investigated the new compounds for possible differing effects toward other P-gp substrates. For this purpose we used the MTT assay to determine the influence of selected modulators on the toxicity of colchicine and vinblastine, two typical cytotoxic P-gp substrates. Finally, we set out to further elucidate their mode of action. Activators of substrate transport could cause conformational changes in the TM domains, increasing the affinity of the substrate to its binding site. Other possible mechanisms of activation would suggest involvement of the nucleotide binding domains (NBDs): 1) acceleration of transport velocity resulting in an increased conversion of ATP, or 2) enhanced affinity of ATP for the NBDs, leading to increased binding. To elucidate the potential involvement of the NBDs in the mechanism of activation, we investigated the influence of two selected activators (compounds **3** and **10**) on drug-stimulated ATPase activity and the affinity of ATP toward P-gp in the presence and absence of these two activators.

Chemistry

Compound **2** was synthesized as described earlier by direct conversion of cyclohexanone **1** with thiourea and iodine.^[15] 5,6,7,8-Tetrahydroimidazo[2,1-*b*]benzothiazoles (Scheme 1) were prepared according to the method of Barchéath et al. without modification.^[16] In contrast, cyclization of the imidazo[1,2-*a*]benzimidazoles (Scheme 2) did not proceed under these conditions, and only the acyclic ethanones could be isolated as iminium salts. The use of acetone instead of ethanol significantly increased the yield and purity of the products.^[17] Cycli-



Scheme 1. Synthesis of 5,6,7,8-tetrahydroimidazo[2,1-*b*]benzothiazoles: a) thiourea, I₂, 110 °C, 12 h; b) BrCH₂COC₆H₄R, EtOH, reflux, 6 h.



Scheme 2. Synthesis of imidazo[1,2-*a*]benzimidazoles: a) NaH, X-R¹, THF, 0 °C, 10 min, then reflux, 12 h; b) BrCH₂COC₆H₄R₂, EtOH, reflux, 3 h (or acetone, RT, 12 h); c) NaOH or K₂CO₃, MeOH, reflux, 12–24 h.

zation was performed without further purification in the presence of a strong base (aqueous sodium hydroxide or potassium carbonate).^[18] The final products were obtained as solids after the addition of water.

Selective alkylation of 2-aminobenzimidazole (**6**) at position N1 was carried out by the use of sodium hydride in THF,^[19] which gave higher yields and fewer byproducts when arylmethyl chlorides were used as educts. Workup was performed by silica gel chromatography to remove excess alkylation reagent. In a first step the side products could be eluted with ethyl acetate, whereas the desired products could only be recovered by elution with methanol.

Results and Discussion

Confirmation of P-gp expression in A2780 Adr cells

The multidrug-resistant A2780 Adr cell line used in this study was obtained by treatment of the human ovarian cancer cell line A2780 with increasing concentrations of doxorubicin (adriamycin).^[20,21] To assure that doxorubicin-selected A2780 Adr cells show a significant overexpression of human P-gp, crude cell membranes of both cell lines were obtained as described in the Experimental Section (below) and were analyzed by SDS PAGE followed by Western blot. By using the monoclonal antibody (mAb) C219,^[22] a band of P-gp could be stained in A2780 Adr samples but not in wild-type A2780 cells (Figure 2a). Crude membranes of CHO-K1 cells stably transfected with the human *abcb1* gene (CHO-K1-MDR1 M403) and human P-gp purified from *Saccharomyces cerevisiae* were used as positive controls. To routinely demonstrate sufficient amounts of the *abcb1* gene product in living cells,^[23] we used antibody staining with the FITC-labeled monoclonal anti-P-gp antibody 17F9, which can be detected directly by flow cytometry. A greater than tenfold increase in fluorescence intensity was measured in A2780 Adr cells (50.01 ± 1.41) relative to A2780 cells (3.67 ± 0.02; equivalent to autofluorescence), also pointing to a significant overexpression of P-gp on the surface of the resistant cells (Figure 2b).

In previous studies we were able to show a good correlation of the inhibitory activities of a series of P-gp modulators in A2780 Adr and MDCK cells stably transfected with the *abcb1*

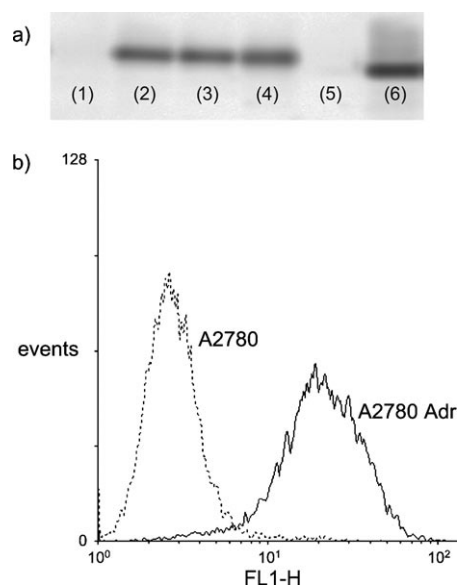


Figure 2. a) Overexpression of P-glycoprotein in A2780 Adr cells was demonstrated by Western blot. In A2780 Adr cells (lanes 2 and 3), a band of P-gp was stained with the mAb C219, whereas wild-type A2780 cells do not contain P-gp (lane 1). CHO-K1 cells stably transfected with the *abc1* gene (lane 4) and human P-gp purified from *S. cerevisiae* (lane 6) were used as positive controls. Due to varying patterns of glycosylation the molecular weight of P-gp purified from yeast is different from that expressed in mammalian cells; the protein size standard (lane 5) is not visible after mAb staining. b) P-gp expression in A2780 Adr could also be detected with the FITC-labeled mAb 17F9 and flow cytometric detection. An exemplary histogram obtained in the flow cytometric measurement is shown. The mean fluorescence values of three replicates are 50.01 ± 1.41 for A2780 Adr cells, and 3.67 ± 1.41 for wild-type cells.

gene (MDCK-MDR1).^[24] Additionally, the absence of other ABC transporters such as BCRP (ABCG2), which recognizes similar substrates, was also proven by antibody staining using BXP-21.^[25–28] Considering all the experimental and published data, we conclude that A2780 Adr, the cell line used in this study, shows a significant overexpression of the *abc1* gene, and thus P-gp is the main factor that mediates active drug efflux in these cells.

Activation of P-gp-mediated efflux and structure–activity relationships

In an initial step the P-gp-modulating properties of QB102 (**3**) and its direct analogues **4** and **5** were investigated in a daunorubicin accumulation assay. For this purpose cells were incubated with DNR in combination with various concentrations of the modulators for three hours to reach steady state. Intracellular DNR fluorescence was subsequently measured by flow cytometry. In the presence of the three benzothiazoles, intracellular fluorescence in A2780 Adr decreased with increasing concentrations of the modulator, indicating enhanced efflux of DNR from the cells. As no effect on wild-type A2780 cells was observed, we conclude that the decrease in fluorescence in A2780 Adr was caused by stimulation of P-gp-mediated efflux rather than nonspecific effects. In previous studies it was postulated that the QB compounds bind to the so-called H site

of P-gp and stimulate transport of R-type substrates such as DNR in a positive cooperative manner,^[14,29] as was initially reported for Hoechst 33342.^[4] Therefore, we also investigated the effect of this substance on intracellular DNR accumulation. However, Hoechst 33342 decreased DNR fluorescence in wild-type A2780 cells as well as in A2780 Adr. A significant decrease by the same amount (50%) was also observed in the absence of any cells (Figure 3a), indicating that the decreased intracel-

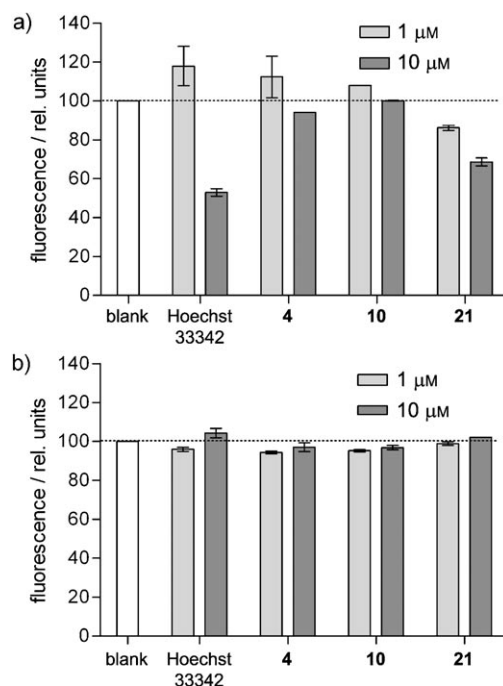


Figure 3. Interaction of selected modulators with a) DNR and b) rho 123 fluorescence. The fluorescence properties of both substrates in the presence or absence of two different modulator concentrations (indicated) were measured after excitation at 485 nm ($\lambda_{em(DNR)} = 590$ nm, $\lambda_{em(\rho 123)} = 520$ nm). Activation of DNR efflux by Hoechst 33342 and **21** cannot be characterized due to fluorescence quenching caused by both substances (a); rho 123 fluorescence is not influenced by any of the compounds (b).

lular fluorescence in the presence of Hoechst 33342 is not due to a stimulation of DNR efflux, but instead an apparent artifact of fluorescence quenching. A similar phenomenon was described by Tang et al. when combinations of DNR and Hoechst 33342 were used for fluorescence-based monitoring of P-gp function.^[30]

To compare the activities of these compounds, concentration–response curves were generated by plotting intracellular DNR fluorescence values versus the logarithmic concentration of the modulator (Figure 4a). The EC_{50} values of the P-gp-activating benzothiazoles calculated from these curves are listed in Table 1. In this group of substances, compound **5** was the most potent activator ($EC_{50} = 0.117 \pm 0.001$ μM) followed by **4** ($EC_{50} = 0.207 \pm 0.055$ μM). Both compounds effected half-maximal activation of P-gp in the high nanomolar concentration range and thus were about five- to tenfold more potent than the parent compound **3** ($EC_{50} = 0.916 \pm 0.045$ μM). As **5** only differs from **3** by the presence of an electron-withdrawing

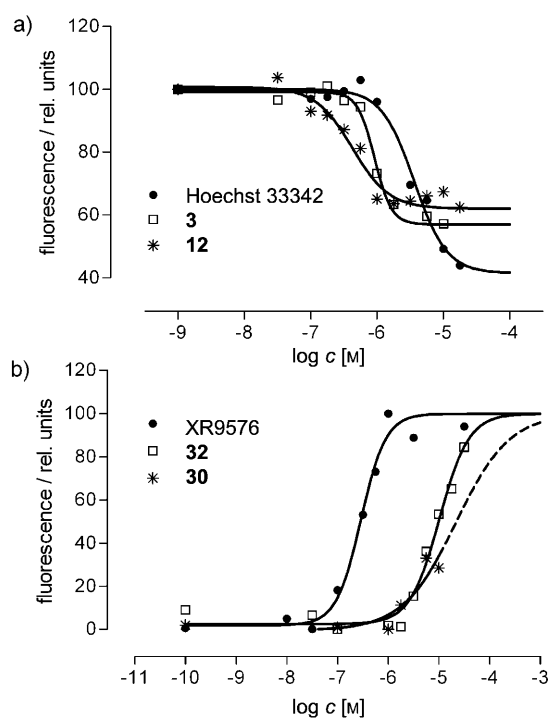


Figure 4. a) Exemplary concentration–response curves of various P-gp activators. The curves were generated in the rho 123 accumulation assay, and EC_{50} values \pm SD were calculated from at least three independent experiments. In this assay **12** is the most potent activator ($EC_{50} = 0.271 \pm 0.027 \mu\text{M}$). Hoechst 33342: $EC_{50} = 3.552 \pm 0.168 \mu\text{M}$; **3**: $EC_{50} = 0.916 \pm 0.045 \mu\text{M}$. b) Exemplary concentration–response curves of P-gp inhibitors obtained in the DNR accumulation assay. IC_{50} values were calculated by nonlinear regression. The imidazobenzimidazoles **32** ($IC_{50} = 7.79 \pm 0.826 \mu\text{M}$) and **30** ($IC_{50} > 10 \mu\text{M}$) provide a significantly lower potency of inhibition than other known P-gp inhibitors such as XR9576 ($IC_{50} = 0.145 \pm 0.003 \mu\text{M}$). A complete concentration–response curve could not be obtained for **30** due to its poor aqueous solubility.

Table 1. P-gp-activating benzothiazoles, with EC_{50} values obtained in the daunorubicin and rhodamine 123 accumulation assays.

Compd	R ¹	EC_{50} [μM] ^[a]	
		DNR	rho 123
3 (QB102)	-CH ₃	0.916 ± 0.045	1.11 ± 0.17
4	-CN	0.207 ± 0.055	1.58 ± 0.16
5	-NO ₂	0.117 ± 0.001	1.36 ± 0.13

[a] EC_{50} values (\pm SD) are the average of at least three independent experiments.

nitro substituent instead of the methyl group at position 4 of the phenyl ring, the electronic properties of this substituent might determine its activity. This hypothesis is supported by the fact that the corresponding benzonitrile **4** is also considerably more potent than **3**.

To further investigate this putative relationship, a second group of compounds structurally related to QB11 (Figure 1 b), another published activator of P-gp, was designed. The *N*-

methylbenzimidazole basic structure was chosen, as it provides a broader range of possibilities for additional structural modifications (e.g., at position N9) than the previously described benzothiazoles. The structures and EC_{50} values of these twelve substances (**9–20**) are summarized in Table 2. In this series, derivatives with electron-withdrawing substituents at positions 3 or 4 of the phenyl ring also showed the strongest modulating activity. Based on this observation an initial structure–activity relationship analysis enclosing the *N*-methylated imidazobenzimidazoles was performed. For *meta*- and *para*-substituted activators—except for **19**—a good correlation between pEC_{50} values and the Hammett substituent constant, σ , was observed. Predicted pEC_{50} values were calculated with the equation: $pEC_{50} = (0.517 \pm 0.077) \sigma + (6.108 \pm 0.036)$. These values showed a significant correlation ($r^2 = 0.86$) with those observed in the DNR accumulation assay (Figure 5).

A direct correlation between overall lipophilicity and P-gp interaction for structurally related substrates or modulators has been described in various published studies.^[31–33] As it was postulated that P-gp substrates can enter the drug binding pocket from the plasma membrane,^[34–36] the accumulation of highly hydrophobic compounds in the membrane bilayer could facilitate drug binding at the protein, resulting in an increased apparent affinity of those substances toward P-gp. To elucidate whether the differences in the activating potency of the *N*-methylimidazobenzimidazoles (**9–20**) can be attributed to differences in their lipophilic properties, we calculated their octanol–water partition coefficients (ACD 5.09, Advanced Chemistry Development Inc., Toronto, Canada). In this group of substances no significant correlation between $\log P_{\text{calcd}}$ and pEC_{50} values obtained in the DNR accumulation assay were observed (Figure 6 a). Considering the close structural relationship of these activators and their similar $\log P_{\text{calcd}}$ values, this observation is not surprising. To further ensure that the different modulating properties are not due to an enhanced partition of hydrophobic compounds into the membrane bilayer, we additionally calculated $\log P$ values for the additional nine activating imidazobenzimidazoles with various *N* substituents (described below). In this group as well, no correlation between lipophilicity and biological activity (rho 123 accumulation assay) was observed, although substances providing a broader range of partition coefficients were included in this analysis (Figure 6 b). In summary, the different activating properties of the novel benzimidazoles are not caused by variable partitioning into the plasma membrane, but rather by different affinities toward P-gp. Therefore, the binding affinity seems—at least in the case of daunorubicin—to depend strongly on the electronic properties of the substituent at the phenyl portion of the activator structure.

To verify that the enhanced efflux of DNR mediated by most of the substances is not a phenomenon specific to this drug or the class of anthracyclines, we tested whether the new compounds are also able to decrease the intracellular accumulation of rhodamine 123, another typical substrate of the so called R site of P-gp. The fluorescence properties of rho 123 were not influenced by any of the substances, including Hoechst 33342. As expected, stimulation of rho 123 efflux was observed in the

Table 2. P-gp-activating benzimidazoles, with EC₅₀ values obtained in the daunorubicin and rhodamine 123 accumulation assays.

Compd	R ¹	R ²	EC ₅₀ [μM] ^[a]	
			DNR	rho 123
9	methyl	H	1.11 ± 0.27	1.43 ± 0.40
10	methyl	4-CN	0.379 ± 0.127	1.09 ± 0.29
11	methyl	4-CH ₃	1.21 ± 0.26	0.977 ± 0.271
12	methyl	4-NO ₂	0.343 ± 0.066	0.271 ± 0.027
13	methyl	3-NO ₂	0.225 ± 0.016	0.305 ± 0.082
14	methyl	4-OCH ₃	1.51 ± 0.45	0.951 ± 0.152
15	methyl	3-OCH ₃	1.27 ± 0.19	0.629 ± 0.104
16	methyl	2-OCH ₃	1.39 ± 0.10	0.545 ± 0.136
17	methyl	3,4-CH=CH-CH=CH-	1.36 ± 0.09	0.463 ± 0.073
18	methyl	4-Cl	0.545 ± 0.086	0.605 ± 0.072
19	methyl	4-NH ₂	1.17 ± 0.07	0.706 ± 0.191
20	methyl	3-NH ₂	0.921 ± 0.245	0.660 ± 0.029
21	benzyl	4-CN	ND ^[b]	0.922 ± 0.150
22	benzyl	4-CH ₃	ND	1.21 ± 0.20
23	benzyl	4-NO ₂	ND	1.20 ± 0.16
24	benzyl	4-OCH ₃	ND	0.253 ± 0.003
25	methallyl	4-CN	1.13 ± 0.27	0.847 ± 0.085
26	4-methoxybenzyl	4-CN	ND	0.876 ± 0.228
27	3,4-difluorobenzyl	4-CN	ND	0.836 ± 0.093
28	3,4-dichlorobenzyl	4-CN	ND	2.23 ± 0.42
29	6-chloro-4H-benzo[1,3]dioxin-8-yl)methyl	4-CN	0.423 ± 0.118	0.245 ± 0.008

[a] EC₅₀ values (±SD) are the average of at least three independent experiments. [b] ND: not determined due to fluorescence quenching.

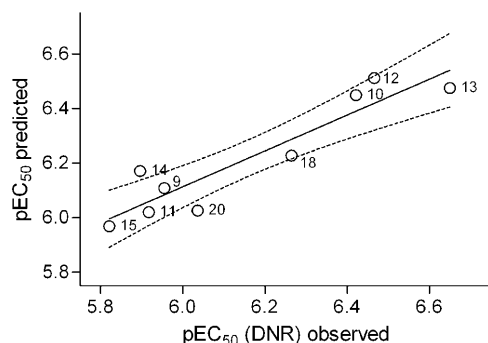


Figure 5. Structure–activity relationships of activators with the imidazobenzimidazole core structure. The activating potency of N-methylated activators correlates with the Hammett σ value of the *meta* or *para* substituent at the phenyl ring. The predicted pEC₅₀ values calculated using the equation $pEC_{50} = (0.517 \pm 0.077)\sigma + (6.108 \pm 0.036)$ show a significant correlation with those observed in the DNR accumulation assay ($r^2 = 0.86$).

presence of activators, and the EC₅₀ values of most of the compounds were in the same approximate range as determined for DNR (Tables 1 and 2). However, the highly potent compounds **4**, **5**, and **10** showed a surprisingly weak activity in this assay, leading to EC₅₀ values similar to the less potent activators. In this drug accumulation assay, Hoechst 33342 was also able to stimulate the efflux of rho 123, but only at higher concentrations than the new QB derivatives (EC₅₀ = 3.55 ± 0.17 μM).

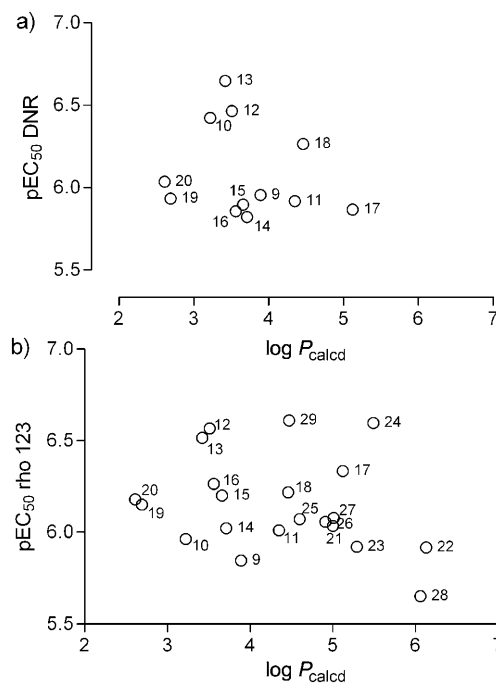


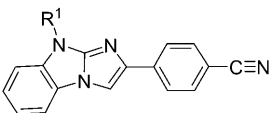
Figure 6. Scatter plot of calculated logP and pEC₅₀ values of P-gp activators. a) The biological activity (DNR accumulation assay) of N-methylated imidazobenzimidazoles **9–20** does not depend on their lipophilicity ($r^2 = 0.04$). b) The pEC₅₀ values obtained in the rho 123 accumulation assay also do not show any correlation with logP values when all of the imidazobenzimidazole-type activators are included ($r^2 = 0.07$).

If the model of Shapiro and Ling^[4] is taken as a basis, the activation of DNR and rho 123 efflux can be explained in terms of a positive cooperativity between the two binding sites. Due to their structural similarity to Hoechst 33342 the activators presumably bind to the H site of the transporter^[29] and cause conformational changes in the TM regions that enhance drug binding at the R site. In the presence of the activators, an approximate twofold stimulation of drug transport was observed which is in the order of magnitude reported by Shapiro and Ling.^[4] Accordingly, the positive cooperative interaction between the two distinct binding sites of the protein previously detected in plasma membrane vesicles can also be shown in a functional assay using entire cells.

Because the imidazobenzothiazoles and N-methylated imi-

dazobenzimidazoles are structurally closely related to the parent compounds QB102 and QB11, it is not surprising that they are also able to activate P-gp. To further explore the influence of structural variations on the activating properties we designed a third series of twelve substances based on the structure of **10**, one of the most potent imidazobenzimidazoles, in which the *N*-methyl group is replaced by bulkier residues (compounds **21–32**). Interestingly these changes greatly altered the modulating potency of the substances. The benzyl derivatives **21–28** still activate P-gp-mediated efflux of rho 123, whereas the influence of these compounds on DNR accumulation could not be measured satisfactorily due to fluorescence quenching (Figure 3a). In contrast, **30**, **32**, and **31**, with two- and three-carbon alkyl linkers, respectively, seemed to weakly inhibit the efflux of DNR (Table 3). According to this observa-

Table 3. Compounds showing weak inhibitory properties, with IC_{50} values obtained in the daunorubicin and rhodamine 123 accumulation assays.



Compd	R ¹	IC ₅₀ [μM] ^[a]	
		DNR	rho 123
30	phenylethyl	> 10.0	–
31	phenylpropyl	> 10.0	–
32	piperidine- <i>N</i> -ethyl	7.79 ± 0.83	13.0 ± 0.4

[a] IC₅₀ values (± SD) are the average of at least three independent experiments.

tion, the size of this substituent or the length of the alkyl linker may also be decisive for the modulating properties. The inhibitory tendency of these three substances may be caused by a differing spatial orientation of the larger *N*-linked substituents preventing either appropriate binding of the modulator to the protein or the conformational changes that are essential for activation. However, these compounds show a significantly lower inhibiting potency than several known inhibitors such as verapamil or XR9576 (Figure 4b), and in most cases complete concentration–response curves could not be obtained due to the poor aqueous solubility of the substances.

The inhibitory effect of **30** and **31** seems to be limited to the transport of DNR, whereas the efflux of rho 123 remains unaffected or is inhibited at very high concentrations, as was observed for **32**. From these observations it can be concluded that although both substrates are postulated to share a unique binding site at the transporter, their explicit binding properties may differ from each other due to their structural diversity. This hypothesis is also supported by the fact that in the group of clearly activating compounds, the correlation of the EC₅₀ values obtained for DNR and rho 123 is only moderate. In summary, the R site of P-gp should rather be considered a “binding region” than a unique “binding site”.^[5,7,37] The localization of the postulated drug binding sites was extensively investigated with various experimental approaches as well as

molecular modeling techniques.^[29,38–40] These regions are presumably collocated in the large internal cavity of the protein formed by the TM region. According to a recently published crystal structure of mouse P-gp, this cavity is large enough to bind several ligands simultaneously, supporting the idea that binding of a molecule at one binding site can enhance the binding of another.^[36]

Effect on other P-gp substrates

Because it was shown that compound **3** has different effects on the cellular accumulation of distinct P-gp substrates, we analyzed whether the newly synthesized derivatives are also able to modulate substrate specificity of P-gp. For this purpose we selected several activators, including **3**, as well as one inhibitor (compound **30**) and investigated their effect on P-gp-mediated resistance to vinblastine and colchicine using the MTT assay. These two drugs were selected, as they are classical P-gp substrates and, according to Kondratov et al.,^[14] their transport is either decreased or remains unaffected by **3**. We initially tested whether the selected substances themselves display any toxicity toward A2780 Adr and wild-type cells. At concentrations up to 10 μM, no significant toxic effects of the test compounds were detected; the cytotoxicity that occurs at higher concentrations is due to the increasing amount of organic solvent required because of the low aqueous solubility of these substances (Figure 7). According to this observation, in the subsequently performed assays a final modulator concentration of 10 μM was combined with varying concentrations of vinblastine and colchicine.

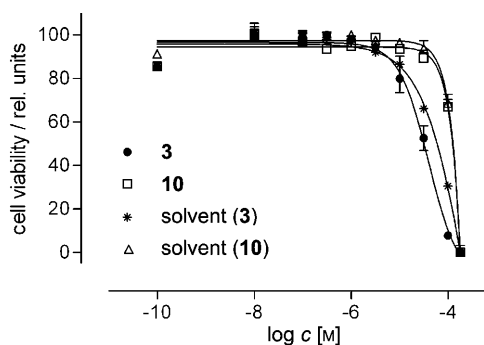


Figure 7. Toxicity of selected activators toward A2780 cells determined in the MTT assay. Both compounds **3** and **10** do not display any cytotoxic effects at concentrations up to 10 μM. Toxicity at higher concentrations is due to the amount of organic solvent (MeOH, DMSO) required, owing to the poor solubility of these compounds. Thus a fixed modulator concentration of 10 μM was used for the subsequent combination assays.

In all MTT assays the toxicity of the cytostatic drugs toward wild-type A2780 cells was not influenced by the newly synthesized compounds as well as **3** at a concentration of 10 μM. All of the modulators were able to decrease the degree of resistance of MDR A2780 Adr cells against vinblastine (Figure 8), probably through inhibition of P-gp-mediated efflux of the cytostatic drug. A different effect was observed in the case colchicine. In accordance with published reports, **3** did not influ-

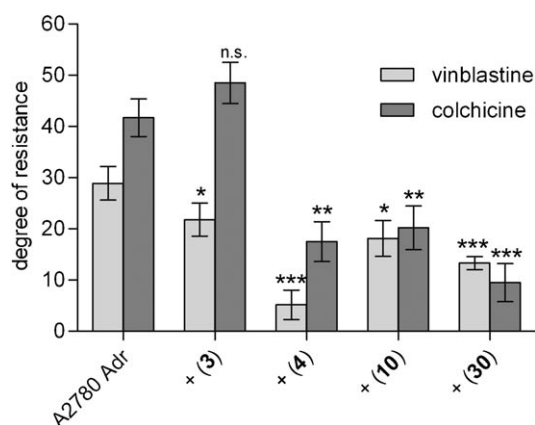


Figure 8. Degree of resistance of P-gp-overexpressing A2780 Adr cells against vinblastine and colchicine in the presence or absence of various modulators (10 μM). The degree of resistance was defined as $F_r = (\text{IC}_{50\text{resistant}}) / (\text{IC}_{50\text{sensitive}})$. Resistance of A2780 Adr against vinblastine is significantly decreased by all of the compounds, including the postulated activators (**3**, **4**, and **10**) as well as the inhibitor **30**. Colchicine resistance is also decreased in the presence of the modulators except for **3**. Statistical significance: * $0.01 < p < 0.005$, ** $0.001 < p < 0.01$, *** $p < 0.001$ (two-tailed t-test); n.s., not significant.

ence colchicine toxicity: the slight increase in the degree of resistance observed is not statistically significant. In contrast, in the presence of the newly synthesized substances the level of resistance against colchicine did not remain unaffected, but was decreased, as was previously demonstrated for vinblastine (Figure 8). Clearly the new compounds are also able to inhibit P-gp-mediated efflux of colchicine. Another interesting observation for colchicine is that in most experiments the percentage decrease in resistance was greater than for vinblastine.

These observations can be explained through the postulated binding properties of the two substrates. According to Shapiro and Ling, colchicine, like Hoechst 33342, belongs to the H-type of P-gp substrates.^[4] This model is also supported by the fact that colchicine is able to stimulate DNR efflux in our functional assay, albeit at much higher concentrations than the newly synthesized activators ($\text{EC}_{50} = 14.5 \pm 3.2 \mu\text{M}$). As substances related to **3** and Hoechst 33342 also seem to share this binding site, the increased toxicity of colchicine and vinblastine in the presence of the modulators is presumably due to a competitive inhibition of their P-gp-mediated transport. However, the efflux of vinblastine, which might have affinity for both postulated binding sites,^[4] seems to be reduced by these compounds to a smaller extent. Taking into account the results of the drug accumulation assay, we conclude that the activating properties of the substances develop especially if they interact with substrates that show a distinct specificity to the R site of P-gp. The gradual differences in the strength of the inhibition between vinblastine and colchicine may result from the fact that colchicine binds exclusively to the H site, whereas vinblastine, possibly due to its size, has affinity for both binding sites. Why QB102 behaves differently and does not influence P-gp-mediated transport of colchicine is a question that cannot be answered satisfactorily at this point. Its effect on colchicine efflux may be too small to be detected in this assay, and a more sensitive method has to be used to elucidate this aspect.

Influence of activators on ATPase activity

The previously presented data implicate that the new modulators interact with binding sites within the TM domains. Besides the postulated positive cooperative interactions between the two binding sites, other mechanisms of activation involving the NBDs are possible, by either increasing turnover of ATP or increased affinity of ATP to the NBDs. To further characterize the interaction of the activators with P-gp we first tested the influence of two selected compounds, **3** and **10**, on the ATPase activity of purified P-gp reconstituted in proteoliposomes. In contrast to verapamil, **3** and **10** were both unable to stimulate basal ATPase activity in a concentration-dependent manner (Figure 9a). Again the activators display a behavior

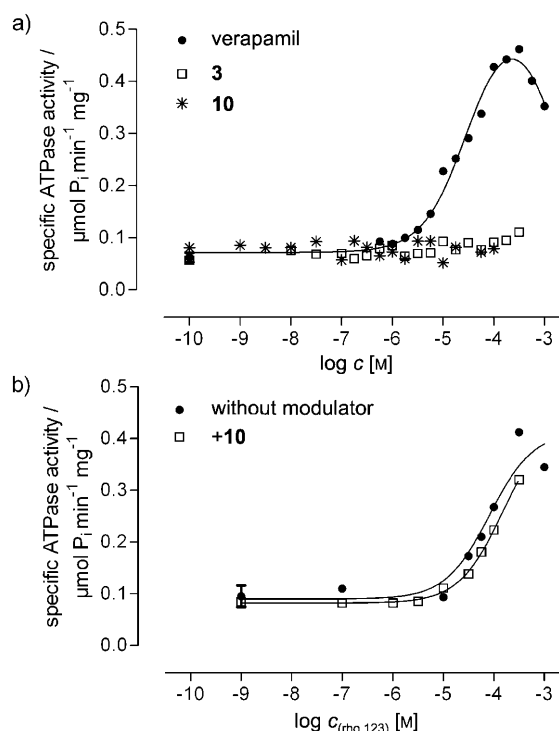


Figure 9. Concentration–response curves of various compounds obtained in the ATPase assay. a) The standard modulator verapamil is able to stimulate the basal ATPase activity of purified P-gp in a concentration-dependent manner. In contrast, the activators **3** and **10** have no effect on ATP hydrolysis. b) Stimulation of the basal ATPase activity by rho 123 is not influenced by **10** at 3.16 μM . $\text{pEC}_{50(\text{rho } 123)} = 4.088 \pm 0.203$, $\text{pEC}_{50(\text{rho } 123 + 10)} = 3.829 \pm 0.040$; (pEC_{50} values \pm SE).

resembling that of Hoechst 33342, which also did not stimulate basal ATPase activity in two published studies.^[41,42] The fluorescent dye rho 123, which was used in the previously described functional assays, is also able to stimulate the basal ATPase activity of P-gp (Figure 9b). As **10** enhanced P-gp-mediated transport of this substrate, we furthermore investigated whether this modulator has any influence on ATPase activity stimulated by rho 123. The fact that **10** does not affect ATPase activity in combination with rho 123 strongly supports the hypothesis that binding of the activators does not accelerate substrate transport by increased conversion of ATP.

As the ATPase activity test is performed with ATP concentrations much higher (10 mM) than physiological conditions, in a second step the influence of **3** and **10** on the affinity of ATP for the protein was analyzed by determination of K_M values for ATP in the presence and absence of these activators. The concentrations of the compounds chosen for this assay had a significant activating effect in the previously described functional assays. In the absence of any drug, we determined a K_M value of 1.08 ± 0.08 mM, which is in the range of values reported previously (for an overview, see reference [43]). The standard modulator verapamil did not influence the affinity of ATP toward the protein which is also in accordance with published data.^[44] In the presence of compound **10** at $0.1 \mu\text{M}$, a slight increase in K_M value for ATP was detected (Table 4). This effect

Table 4. K_M and v_{max} values for the ATPase reaction of P-gp in the presence or absence of **3** and **10**. Verapamil was used as a positive control.

Compd	c [μM]	K_M [$^{\text{a}}$] [mM]	v_{max} [$^{\text{a}}$] [$\mu\text{g P}_i \text{min}^{-1} \text{mg}^{-1}$]
–	–	1.08 ± 0.08	0.052 ± 0.016
verapamil	130	1.056 ± 0.004	0.391 ± 0.015
10	0.100	2.60 ± 0.05	0.086 ± 0.008
	0.316	1.92 ± 0.01	0.069 ± 0.001
	3.16	1.06 ± 0.09	0.062 ± 0.011
3	1.00	1.462 ± 0.151	0.083 ± 0.025
	3.16	1.000 ± 0.365	0.050 ± 0.012

[a] K_M and v_{max} values (\pm SD) represent the average of at least three independent experiments.

was regressive as the concentration of the modulator increased, with a value similar to the basal ATPase activity at the highest concentration of $3.16 \mu\text{M}$. A similar effect was observed for **3**, although to a lesser extent than for **10**. These results show that the mechanism of activation cannot be explained by enhanced affinity of ATP for the transporter. Considering all results from the ATPase measurements, the NBDs are not implicated in the mechanism of activation. This hypothesis is supported by data obtained in the drug accumulation assays. If only conversion of ATP by the NBDs was decisive for P-gp function, the slightly decreased affinity of ATP toward the protein should result in a diminished transport activity in the functional assay. As we observed an enhanced transport of rho 123 and DNR, the previously postulated conformational changes in the TM domains leading to increased affinity of the transported substrate to its binding site are most likely.

Conclusions

The presented data from functional assays show that most of the compounds synthesized in this study display different effects on the intracellular accumulation of various P-gp substrates. Interestingly, the kind of effect seems to depend on the binding site of the substrate. The efflux of rhodamine 123 and daunorubicin, two classical substrates of the R site, is stimulated by most of the compounds. In contrast, the toxicity

of vinblastine and colchicine is increased, indicating an inhibition of P-gp-mediated transport of these drugs belonging to the H-type of substrates. According to this observation, it is possible to conclude that the substances bind to the H site of P-gp and compete for binding with the other substrate. Binding of a modulator to the H site may also stimulate transport at the other postulated binding site in a positive cooperative manner. Thus the positive cooperativity between the two distinct sites for drug transport previously observed in plasma membrane vesicles can also be shown in a functional whole-cell assay. The hypothesis that the enhanced transport of particular substrates is due to conformational changes in the TM region of P-gp leading to enhanced affinity of the substrate toward its binding site is confirmed by the fact that the activators neither influence conversion of ATP nor its affinity for the protein. Regarding these results, we conclude that other mechanisms of activation, which would imply the involvement of the NBDs, are not likely. Because the question of interactions between the multiple functional binding sites of P-glycoprotein, one of the most relevant ABC transporters, could not be answered satisfactorily until now, this series of P-gp modulators is a useful tool to further investigate these mechanisms.

Experimental Section

Chemistry

Educts (e.g., 2-bromoacetophenones, 1-methylbenzimidazole-2-amine, 1-benzylbenzimidazole-2-amine) and reagents were obtained from commercial sources (Acros Organics, Alfa Aesar, Sigma–Aldrich, or Maybridge) and were used without any purification. Spectral data were obtained on the following instruments: ^1H NMR, Bruker Advance 500 (500 MHz); ^{13}C NMR, Bruker Advance 500 (125.8 MHz). The ^{13}C NMR signals were assigned with the aid of distortionless enhancement by polarization transfer (DEPT), attached proton test (APT), and two-dimensional experiments (HSQC, HMBC); classification of carbon atoms are indicated by CH_3 (primary), CH_2 (secondary), CH or Ar-CH (tertiary), or Ar-C (quaternary); J values are given in Hz; multiplicity of resonance peaks is indicated as singlet (s), doublet (d), doublet from doublet (dd), triplet (t), doublet from triplet (dt), quartet (q), quintet (q), and multiplet (m). IR spectra were recorded on a Bruker Alpha-P instrument. ESI Fourier-transform ion cyclotron mass spectrometry was performed in the positive-ion mode using a high-resolution APEX-QE instrument (Bruker Daltonics, USA). Elemental analyses were performed on a Vario EL instrument from Elementar. Determined values were all within $\pm 0.4\%$ of the theoretical values except where indicated.

Method A: Synthesis of N1-substituted benzimidazoles. A solution of 2-aminobenzimidazole (1 equiv) in THF (5 mL mmol^{-1}) was stirred at 0°C with NaH (60% in mineral oil, 1.3 equiv). After 10 min, the appropriate alkyl halide (1.2 equiv) dissolved in THF was added dropwise at 0°C . The mixture was then heated at reflux for 12 h. The reaction mixture was cooled to room temperature, diluted with EtOAc, and washed three times with 1 M NaOH. The organic layer was concentrated under reduced pressure. The residue was purified by column chromatography using silica and EtOAc as eluent. The desired compound was eluted from the column with MeOH. The eluate was evaporated, and the residue was treated with a small quantity of THF and thereafter with excess *n*-hexane.

The compound was obtained as a solid, and was washed with *n*-hexane and dried.

Method B: Synthesis of acyclic ethanones. A suitably substituted 2-bromoacetophenone (1 equiv) was added to a solution of an N1-substituted 2-aminobenzimidazole (1 equiv) in EtOH (60 mL mmol⁻¹) and heated at reflux for 3 h and then cooled to room temperature; alternatively, acetone (50 mL mmol⁻¹) was used at room temperature for 12 h. The compound was obtained as a hydrobromide, which was separated, washed, and dried.

Method C: Synthesis of imidazo[1,2-*a*]benzimidazoles. The acyclic ethanone was dissolved in MeOH (~100 mL mmol⁻¹), and 1 M NaOH (one third volume) or solid K₂CO₃ (in excess) was added. The reaction mixture was heated at reflux for 12–24 h. The solution was cooled to room temperature, concentrated, and the residue was treated with H₂O. The compound was obtained as a solid product, which was separated, washed with H₂O, and dried.

Method D: Synthesis of imidazo[2,1-*b*]thiazoles. A suitable 2-bromoacetophenone (1 equiv) was added to a stirred solution of a 2-aminothiazole (1 equiv) in EtOH (~50 mL mmol⁻¹) and heated at reflux for 6 h. The reaction mixture was cooled to room temperature, and the compound was obtained as a solid product, which was separated, washed with EtOH, and dried.

4,5,6,7-Tetrahydrobenzothiazol-2-amine (2). Compound **2** was synthesized as described by Zhu et al.^[15]

1-Phenylethylbenzimidazol-2-amine (7a). According to method A, **6** (1.33 g, 10.0 mmol) and 2-phenylethylbromide (2.41 g, 13.0 mmol) were reacted, and compound **7a** was obtained as a brown solid (1.21 g, 51.0%): reference [45].

1-(2-Methylallyl)benzimidazol-2-amine (7b). According to method A, **6** (1.33 g, 10.0 mmol) and 1-methylallylchloride (1.36 g, 15.0 mmol) were reacted, and compound **7b** was obtained as a white solid (0.956 g, 51%): ¹H NMR (500 MHz, [D₆]DMSO): δ = 7.09–7.16 (m, 1H), 6.99–7.05 (m, 1H), 6.92 (dt, *J* = 7.6, 1.3 Hz, 1H), 6.84 (dt, *J* = 7.4, 1.0 Hz, 1H), 6.34 (brs, 2H), 4.82 (qi, *J* = 1.3 Hz, 1H), 4.54 (s, 2H), 4.52 (q, *J* = 0.8 Hz, 1H), 1.66 ppm (d, *J* = 0.5 Hz, 3H); ¹³C NMR (125 MHz, [D₆]DMSO): δ = 154.2, 142.9, 140.5, 134.5, 120.4, 118.1, 114.8, 111.1, 107.9, 47.1, 19.8 ppm; HRMS-ESI: *m/z* [M]⁺ calcd for C₁₁H₁₃N₃: 187.1109, found: 187.1110.

1-(3-Phenylpropyl)benzimidazol-2-amine (7c). According to method A, **6** (1.33 g, 10.0 mmol) and 3-phenylpropylbromide (2.99 g, 15.0 mmol) were reacted, and compound **7c** was obtained as a brown solid (0.301 g, 12%): ¹H NMR (500 MHz, [D₆]DMSO): δ = 7.24–7.29 (m, 2H), 7.15–7.18 (m, 3H), 7.09–7.14 (m, 1H), 7.11 (d, *J* = 7.7 Hz, 1H), 7.04 (d, *J* = 7.3 Hz, 1H), 6.91 (dt, *J* = 7.5, 1.1 Hz, 1H), 6.84 (dt, *J* = 7.5, 1.1 Hz, 1H), 6.36 (brs, 2H), 4.00 (t, *J* = 7.3 Hz, 2H), 2.61 (t, *J* = 8.5 Hz, 2H), 1.92 ppm (qi, *J* = 7.3 Hz, 2H); ¹³C NMR (125 MHz, [D₆]DMSO): δ = 154.9, 143.0, 141.5, 134.4 (Ar-C), 128.5 (2C), 128.2 (2C), 126.00, 120.3, 118.0, 114.8, 107.4, 41.4, 32.4, 30.4 ppm; HRMS-ESI: *m/z* [M]⁺ calcd for C₁₆H₁₇N₃: 251.1422, found: 251.1421.

1-(4-Methoxybenzyl)benzimidazol-2-amine (7d). According to method A, **6** (1.33 g, 10.0 mmol) and 4-methoxybenzylchloride (2.04 g, 13.0 mmol) were reacted, and compound **7d** was obtained as a pale-pink solid (1.47 g, 58%): reference [46].

1-(3,4-Difluorobenzyl)benzimidazol-2-amine (7e). According to method A, **6** (1.33 g, 10.0 mmol) and 3,4-difluorobenzylchloride (2.11 g, 13.0 mmol) were reacted, and compound **7e** was obtained as a white solid (1.61 g, 62%): ¹H NMR (500 MHz, [D₆]DMSO): δ = 7.32–7.40 (m, 1H), 7.22–7.31 (m, 1H), 7.14 (d, *J* = 7.7 Hz, 1H), 7.08

(d, *J* = 7.6 Hz, 1H), 6.98–7.02 (m, 1H), 6.93 (dt, *J* = 7.7, 1.2 Hz, 1H), 6.83 (dt, *J* = 7.6, 1.0 Hz, 1H), 6.57 (brs, 2H), 5.24 ppm (s, 2H); ¹³C NMR (125 MHz, [D₆]DMSO): δ = 155.0, 150.1 (dd, *J* = 78.3, 12.7 Hz), 143.1, 148.1 (dd, *J* = 77.5, 12.7 Hz), 135.2 (dd, *J* = 4.9, 3.9 Hz), 134.1, 124.0 (dd, *J* = 6.5, 3.4 Hz), 120.8, 118.4, 117.8 (d, *J* = 17.1 Hz), 115.3 (d, *J* = 17.4 Hz), 115.1, 108.0, 43.9 ppm; HRMS-ESI: *m/z* [M]⁺ calcd for C₁₄H₁₁F₂N₃: 259.0921, found: 259.0920.

1-(3,4-Dichlorobenzyl)benzimidazol-2-amine (7f). According to method A, **6** (1.33 g, 10.0 mmol) and 3,4-dichlorobenzylchloride (2.54 g, 13.0 mmol) were reacted, and compound **7f** was obtained as a white solid (1.59 g, 65.4%): reference [47].

1-(2-(Piperidin-1-yl)ethyl)benzimidazol-2-amine (7g). According to method A, **6** (1.33 g, 10.0 mmol) and 1-(2-chloroethyl)piperidine (1.92 g, 13.0 mmol) were reacted, and compound **7g** was obtained as a white solid (1.61 g, 62%): reference [48].

1-{(6-Chloro-4*H*-benzo[1,3]dioxin-8-yl)methyl}benzimidazol-2-amine (7h). According to method A, **6** (0.53 g, 4.0 mmol) and 6-chloro-8-(chloromethyl)-4*H*-benzo[1,3]dioxin (1.14 g, 4.8 mmol) were reacted, and compound **7h** was obtained as a brown solid (0.62 g, 49%): ¹H NMR (500 MHz, [D₆]DMSO): δ = 7.16 (d, *J* = 7.8 Hz, 1H), 7.09 (s, 1H), 6.92–6.99 (m, 2H), 6.80–6.85 (m, 1H), 6.47 (m, 3H), 5.38 (s, 2H), 5.17 (s, 2H), 4.90 ppm (s, 2H); ¹³C NMR (125 MHz, [D₆]DMSO): δ = 155.2, 148.7, 143.0, 134.1, 126.7, 124.8, 124.6, 124.4, 123.7, 120.9, 118.4, 115.1, 107.8, 91.4, 65.3, 39.4 ppm; HRMS-ESI: *m/z* [M]⁺ calcd for C₁₆H₁₄ClN₃O₂: 315.0775, found: 315.0775.

2-(2,3-Dihydro-2-imino-3-methyl-1*H*-benzimidaz-1-yl)-1-phenylethanone hydrobromide (8a). According to method B, 1-methylbenzimidazole-2-amine (0.74 g, 5.0 mmol) and 2-bromoacetophenone (1.23 g, 5.5 mmol) were dissolved in acetone, and compound **8a** was obtained as a white solid (1.98 g, 57%): Anal. calcd for C₁₆H₁₆BrN₃O: C 55.52, H 4.66, N 12.14, found: C 55.25, H 4.91, N 11.92; reference [49].

4-(2-(2,3-Dihydro-2-imino-3-methyl-1*H*-benzimidaz-1-yl)acetyl)benzimidazole hydrobromide (8b). According to method B, 1-methylbenzimidazole-2-amine (1.47 g, 10.0 mmol) and 2-bromo-4'-cyanoacetophenone (2.24 g, 10.0 mmol) were dissolved in acetone, and compound **8b** was obtained as a white solid (1.21 g, 64%): ¹H NMR (500 MHz, [D₆]DMSO): δ = 8.90 (s, 2H), 8.24 (d, *J* = 8.5 Hz, 2H), 8.13 (d, *J* = 8.5 Hz, 2H), 7.65 (d, *J* = 7.9 Hz, 1H), 7.61 (d, *J* = 7.9 Hz, 1H), 7.36 (dt, *J* = 7.7, 1.0 Hz, 1H), 7.29 (dt, *J* = 7.4, 1.0 Hz, 1H), 6.04 (s, 2H), 3.74 ppm (s, 3H); ¹³C NMR (125 MHz, [D₆]DMSO): δ = 191.1, 150.7, 137.4, 132.9, 130.3, 130.2, 129.2, 123.9, 123.7, 118.2, 116.1, 110.7, 110.5, 50.5, 29.9 ppm; HRMS-ESI: *m/z* [M]⁺ calcd for C₁₇H₁₄N₄O: 290.1168, found: 290.1169; Anal. calcd for C₁₇H₁₅BrN₄O·0.25H₂O: C 54.34, H 4.16, N 14.91, found: C 54.44, H 4.01, N 14.81.

2-(2,3-Dihydro-2-imino-3-methyl-1*H*-benzimidaz-1-yl)-1-(4-methylphenyl)ethanone hydrobromide (8c). According to method B, 1-methylbenzimidazole-2-amine (0.74 g, 5.0 mmol) and 2-bromo-4'-methylacetophenone (1.07 g, 5.0 mmol) were held at reflux in EtOH, and compound **8c** was obtained as a white solid (0.434 g, 24%): Anal. calcd for C₁₇H₁₈BrN₃O: C 56.68, H 5.04, N 11.66, found: C 56.34, H 5.06, N 11.88; reference [50].

2-(2,3-Dihydro-2-imino-3-methyl-1*H*-benzimidaz-1-yl)-1-(4-nitrophenyl)ethanone hydrobromide (8d). According to method B, 1-methylbenzimidazole-2-amine (0.74 g, 5.0 mmol) and 2-bromo-4'-nitroacetophenone (1.21 g, 5.0 mmol) were held at reflux in EtOH, and compound **8d** was obtained as a white solid (0.404 g, 19%): Anal. calcd for C₁₆H₁₅BrN₄O₃·0.33EtOH: C 48.52, H 4.32, N 13.58, found: C 48.61, H 4.28, N 13.34; reference [51].

2-(2,3-Dihydro-2-imino-3-methyl-1H-benzimidaz-1-yl)-1-(3-nitrophenyl)ethanone hydrobromide (8e). According to method B, 1-methylbenzimidazole-2-amine (0.74 g, 5.0 mmol) and 2-bromo-3'-nitroacetophenone (1.21 g, 5.0 mmol) were dissolved in acetone, and compound **8e** was obtained as a white solid (1.46 g, 75%): Anal. calcd for $C_{16}H_{15}BrN_3O_3 \cdot 0.75H_2O$: 47.48, H 4.11, N 13.48, found: C 47.13, H 4.19, N 13.94; reference [51].

2-(2,3-Dihydro-2-imino-3-methyl-1H-benzimidaz-1-yl)-1-(3-methoxyphenyl)ethanone hydrobromide (8f). According to method B, 1-methylbenzimidazole-2-amine (0.74 g, 5.0 mmol) and 2-bromo-3'-methoxyacetophenone (1.14 g, 5.0 mmol) were held at reflux in EtOH, and compound **8f** was obtained as a white solid (0.996 g, 52%): 1H NMR (500 MHz, $[D_6]DMSO$): δ = 8.86 (s, 2H), 7.69 (d, J = 8.2 Hz, 1H), 7.54–7.63 (m, 4H), 7.32–7.38 (m, 2H), 7.30 (dt, J = 7.9, 1.0 Hz, 1H), 6.00 (s, 2H), 3.86 (s, 3H), 3.74 ppm (s, 3H); ^{13}C NMR (125 MHz, $[D_6]DMSO$): δ = 191.2, 159.6, 135.5, 130.3, 130.3, 130.2, 123.8, 123.7, 121.1, 120.3, 113.4, 110.6, 110.5, 55.7, 50.2, 29.8 ppm; HRMS-ESI: m/z $[M]^+$ calcd for $C_{17}H_{17}N_3O_2$: 295.1321, found: 295.1321; Anal. calcd for $C_{17}H_{18}BrN_3O_2 \cdot 0.2H_2O$: C 53.75, H 4.88, N 11.06, found: C 53.79, H 4.80, N 11.14.

2-(2,3-Dihydro-2-imino-3-methyl-1H-benzimidaz-1-yl)-1-(4-methoxyphenyl)ethanone hydrobromide (8g). According to method B, 1-methylbenzimidazole-2-amine (1.33 g, 10 mmol) and 2-bromo-4'-methoxyacetophenone (2.30 g, 10.0 mmol) were dissolved in acetone, and compound **8g** was obtained as a white solid (1.35 g, 70%): 1H NMR (500 MHz, $[D_6]DMSO$): δ = 8.83 (s, 2H), 8.06 (d, J = 9.0 Hz, 2H), 7.60 (d, J = 7.5 Hz, 1H), 7.56 (d, J = 8.0 Hz, 1H), 7.36 (dt, J = 7.5, 1.0 Hz, 1H), 7.27 (dt, J = 7.5, 1.0 Hz, 1H), 7.16 (d, J = 9.0 Hz, 2H), 5.93 (s, 2H), 3.89 (s, 3H), 3.73 ppm (s, 3H); ^{13}C NMR (125 MHz, $[D_6]DMSO$): δ = 189.6, 164.2, 150.9, 131.0 (2C), 130.3, 130.3, 127.1, 123.7, 123.7, 114.3 (2C), 110.6, 110.4, 55.9, 49.6, 29.8 ppm; HRMS-ESI: m/z $[M]^+$ calcd for $C_{17}H_{17}N_3O_2$: 295.1321, found: 295.1318; Anal. calcd for $C_{17}H_{18}BrN_3O_2 \cdot 0.5H_2O$: C 53.00, H 4.97, N 10.91, found: C 53.39, H 5.34, N 10.73.

2-(2,3-Dihydro-2-imino-3-methyl-1H-benzimidaz-1-yl)-1-(2-methoxyphenyl)ethanone hydrobromide (8h). According to method B, 1-methylbenzimidazole-2-amine (1.33 g, 10 mmol) and 2-bromo-2'-methoxyacetophenone (2.30 g, 10.0 mmol) were dissolved in acetone, and compound **8h** was obtained as a white solid (1.76 g, 47%): 1H NMR (500 MHz, $[D_6]DMSO$): δ = 8.85 (s, 2H), 7.84 (dd, J = 7.9, 1.9 Hz, 1H), 7.70 (dt, J = 7.1, 1.6 Hz, 1H), 7.60 (d, J = 7.9 Hz, 1H), 7.54 (d, J = 7.9 Hz, 1H), 7.34 (t, J = 8.2 Hz, 2H), 7.27 (t, J = 7.9 Hz, 1H), 7.11 (t, J = 7.9 Hz, 1H), 5.69 (s, 2H), 4.05 (s, 3H), 3.74 ppm (s, 3H); ^{13}C NMR (125 MHz, $[D_6]DMSO$): δ = 191.0, 160.3, 150.8, 136.0, 130.4, 130.3, 123.7, 123.7, 123.7, 120.8, 113.2, 110.6, 110.4, 56.4, 53.6, 29.8 ppm; HRMS-ESI: m/z $[M]^+$ calcd for $C_{17}H_{17}N_3O_2$: 295.1321, found: 295.1319; Anal. calcd for $C_{17}H_{18}BrN_3O_2$: C 54.27, H 4.82, N 11.17, found: C 54.26, H 4.97, N 11.19.

2-(2,3-Dihydro-2-imino-3-methyl-1H-benzimidaz-1-yl)-1-(napht-2-yl)ethanone hydrobromide (8i). According to method B, 1-methylbenzimidazole-2-amine (0.74 g, 5 mmol) and 2-bromo- α -acetophenone (1.25 g, 5.0 mmol) were dissolved in acetone, and compound **8i** was obtained as a white solid (1.44 g, 72%): 1H NMR (500 MHz, $[D_6]DMSO$): δ = 8.95 (s, 2H), 8.91 (s, 1H), 8.22 (d, J = 7.9 Hz, 1H), 8.13 (d, J = 8.8 Hz, 1H), 8.06 (t, J = 8.1 Hz, 2H), 7.74 (t, J = 7.9 Hz, 1H), 7.70 (t, J = 7.4 Hz, 1H), 7.66 (d, J = 7.9 Hz, 1H), 7.63 (d, J = 7.9 Hz, 1H), 7.38 (t, J = 7.9 Hz, 1H), 7.31 (t, J = 7.6 Hz, 1H), 6.18 (s, 2H), 3.77 ppm (s, 3H); ^{13}C NMR (125 MHz, $[D_6]DMSO$): δ = 191.3, 150.9, 135.6, 132.1, 131.5, 131.0, 130.3 (2C), 129.8, 129.3, 128.6, 128.0, 127.4, 123.8, 123.7, 123.7, 110.6, 110.5, 50.3, 29.9 ppm;

HRMS-ESI: m/z $[M]^+$ calcd for $C_{20}H_{17}N_3O$: 315.1372, found: 315.1371; Anal. calcd for $C_{20}H_{18}BrN_3O_2 \cdot 0.2H_2O$: C 60.07, H 4.64, N 10.51, found: C 59.82, H 4.67, N 10.78.

1-(4-Chlorophenyl)-2-(2,3-dihydro-2-imino-3-methyl-1H-benzimidaz-1-yl)ethanone hydrobromide (8j). According to method B, 1-methylbenzimidazole-2-amine (0.37 g, 2.5 mmol) and 2-bromo-4'-chloroacetophenone (0.61 g, 2.6 mmol) were dissolved in acetone, and compound **8j** was obtained as a white solid (0.76 g, 80%): 1H NMR (500 MHz, $[D_6]DMSO$): δ = 8.85 (s, 2H), 8.10 (d, J = 8.5 Hz, 2H), 7.73 (d, J = 8.5 Hz, 2H), 7.61 (d, J = 7.9 Hz, 2H), 7.35 (t, J = 7.9 Hz, 1H), 7.29 (t, J = 7.6 Hz, 1H), 5.98 (s, 2H), 3.73 ppm (s, 3H); ^{13}C NMR (125 MHz, $[D_6]DMSO$): δ = 190.58, 150.8, 139.3, 132.9, 130.5 (2C), 130.3, 130.2, 129.1 (2C), 123.8, 123.7, 110.6, 110.5, 50.1, 29.8 ppm; HRMS-ESI: m/z $[M]^+$ calcd for $C_{16}H_{14}ClN_3O$: 299.0825, found: 299.0825; Anal. calcd for $C_{16}H_{15}BrClN_3O$: C 50.48, H 3.97, N 11.04, found: C 50.54, H 3.94, N 10.91.

4-(2-(2,3-Dihydro-3-benzyl-2-imino-1H-benzimidaz-1-yl)acetyl)benzonitrile hydrobromide (8k). According to method B, **6** (0.22 g, 1.0 mmol) and 2-bromo-4'-cyanoacetophenone (0.25 g, 1.1 mmol) were dissolved in acetone, and compound **8k** was obtained as a white solid (0.35 g, 78%); Anal. calcd for $C_{23}H_{19}BrN_4O \cdot 0.2H_2O$: C 61.26, H 4.34, N 12.42, found: C 61.18, H 4.64, N 12.26; reference [52].

2-(2,3-Dihydro-3-benzyl-2-imino-1H-benzimidaz-1-yl)-1-(4-methylphenyl)ethanone hydrobromide (8l). According to method B, **6** (1.00 g, 4.5 mmol) and 2-bromo-4'-methylacetophenone (1.07 g, 5.0 mmol) were dissolved in acetone, and compound **8l** was obtained as a white solid (0.856 g, 39%): 1H NMR (500 MHz, $[D_6]DMSO$): δ = 9.07 (brs, 2H), 8.00 (d, J = 8.0 Hz, 2H), 7.61–7.66 (m, 1H), 7.49–7.52 (m, 1H), 7.46 (d, J = 8.0 Hz, 2H), 7.40 (t, J = 7.4 Hz, 2H), 7.34 (t, J = 6.9 Hz, 3H), 7.26–7.31 (m, 2H), 6.02 (s, 2H, CH_2), 5.57 (s, 2H), 2.44 ppm (s, 3H); ^{13}C NMR (125 MHz, $[D_6]DMSO$): δ = 190.8, 150.9, 145.1, 134.6, 131.7 (2C), 130.5, 129.5 (2C), 129.0 (2C), 128.7 (2C), 128.2, 127.0 (2C), 124.0 (2C), 111.0, 110.8, 50.1, 45.7, 21.5 ppm; HRMS-ESI: m/z $[M]^+$ calcd for $C_{23}H_{21}N_3O$: 355.1685, found: 355.1685; Anal. calcd for $C_{23}H_{22}BrN_3O \cdot 0.2H_2O$: C 62.79, H 5.13, N 9.55, found: C 62.71, H 5.26, N 9.62.

2-(2,3-Dihydro-3-benzyl-2-imino-1H-benzimidaz-1-yl)-1-(4-nitrophenyl)ethanone hydrobromide (8m). According to method B, **6** (0.51 g, 2.3 mmol) and 2-bromo-4'-nitroacetophenone (0.67 g, 3.0 mmol) were reacted, and compound **8m** was obtained as a white solid (1.05 g, 98%): 1H NMR (500 MHz, $[D_6]DMSO$): δ = 9.12 (brs, 2H), 8.47 (d, J = 8.9 Hz, 2H), 8.34 (d, J = 9.2 Hz, 2H), 7.69–7.72 (m, 1H), 7.50–7.54 (m, 1H), 7.39–7.43 (m, 2H), 7.30–7.35 (m, 5H), 6.12 (s, 2H), 5.57 ppm (s, 2H); ^{13}C NMR (125 MHz, $[D_6]DMSO$): δ = 190.8, 150.8, 150.6, 138.8, 134.6, 130.4, 130.1 (2C), 129.5, 129.1 (2C), 128.3, 127.1 (2C), 124.1 (2C), 124.0 (2C), 111.0 (2C), 50.8, 45.8 ppm; HRMS-ESI: m/z $[M]^+$ calcd for $C_{22}H_{18}N_4O_3$: 386.1379, found: 386.1392; Anal. calcd for $C_{22}H_{19}BrN_4O_3$: C 56.54, H 4.10, N 11.99, found: C 56.30, H 4.29, N 11.76.

2-(4-Methylphenyl)-5,6,7,8-tetrahydroimidazo[2,1-b]benzothiazole (3). According to method D, **2** (1.45 g, 10 mmol) reacted with 2-bromo-4'-methylacetophenone (2.14 g, 10 mmol) in 150 mL EtOH. The solvent was concentrated, and compound **3** was obtained as a white solid (0.785 g, 28%): HRMS-ESI: m/z $[M]^+$ calcd for $C_{16}H_{16}N_2S$: 279.0830, found: 279.0825; Anal. calcd for $C_{16}H_{16}N_2S \cdot 0.5H_2O$: C 69.28, H 6.18, N 10.10 found: C 69.46, H 6.46, N 9.97; reference [53].

4-(5,6,7,8-Tetrahydroimidazo[1,2-b]benzothiaz-2-yl)benzonitrile (4). According to method D, **2** (0.39 g, 2.5 mmol) reacted with 2-

bromo-4'-cyanoacetophenone (0.56 g, 2.5 mmol) in 150 mL EtOH. The solvent was concentrated, and compound **4** was obtained as gray needles (0.087 g, 12%): HRMS-ESI: m/z $[M]^+$ calcd for $C_{16}H_{13}N_3S$: 279.0830, found: 279.0825; Anal. calcd for $C_{16}H_{13}N_3S \cdot 0.17H_2O$: C 68.08, H 4.76, N 14.88, found: C 68.03, H 4.69, N 14.70; reference [16].

2-(4-Nitrophenyl)-5,6,7,8-tetrahydroimidazo[2,1-*b*]benzothiazole (5). According to method D, **2** (0.39 g, 2.5 mmol) reacted with 2-bromo-4'-nitroacetophenone (0.61 g, 2.5 mmol) in 150 mL EtOH. The solvent was concentrated, and compound **5** was obtained as yellow needles (0.050 g, 7%): HRMS-ESI: m/z $[M]^+$ calcd for $C_{15}H_{13}N_3O_2S$: 299.0728, found: 299.0722; Anal. calcd for $C_{15}H_{13}N_3O_2S \cdot 0.2H_2O$: C 59.47, H 4.46, N 13.87, found: C 59.76, H 4.73, N 13.66; reference [16].

9-Methyl-2-phenyl-9H-imidazo[1,2-*a*]benzimidazole (9). According to method C, **8a** (1.73 g, 5 mmol) was dissolved in MeOH with K_2CO_3 . Compound **9** was obtained as a brown resinous solid (0.962 g, 77%): HRMS-ESI: m/z $[M]^+$ calcd for $C_{16}H_{13}N_3$: 247.1109, found: 247.1110; Anal. calcd for $C_{16}H_{13}N_3 \cdot 0.25H_2O$: C 76.32, H 5.40, N 16.69, found: C 76.29, H 5.52, N 16.39; reference [51].

4-(9-Methyl-9H-imidazo[1,2-*a*]benzimidaz-2-yl)benzonitrile (10). According to method C, **8b** (0.15 g, 0.4 mmol) was dissolved in a mixture of MeOH and 1 M NaOH. Compound **10** was obtained as white needles (0.084 g, 75%): 1H NMR (500 MHz, $[D_6]DMSO$): δ = 8.41 (s, 1H), 8.01 (d, J = 8.6 Hz, 2H), 7.81 (d, J = 8.5 Hz, 2H), 7.76 (d, J = 7.6 Hz, 1H), 7.54 (d, J = 7.9 Hz, 1H), 7.35 (dt, J = 8.0, 1.5 Hz, 1H), 7.22 (dt, J = 7.7, 0.6 Hz, 1H), 3.75 ppm (s, 3H); ^{13}C NMR (125 MHz, $[D_6]DMSO$): δ = 150.2, 141.5, 139.8, 136.3, 132.7 (2C), 125.1 (2C), 123.9, 123.8, 120.3, 119.3, 111.5, 110.4, 108.5, 105.7, 29.2 ppm; IR (ATR): $\tilde{\nu}$ = 2219, 1606, 1493, 1438, 1396, 1109, 1059, 856, 835, 745, 688, 544, 436 cm^{-1} ; HRMS-ESI: m/z $[M]^+$ calcd for $C_{17}H_{12}N_4$: 272.1062, found: 272.1064; Anal. calcd for $C_{17}H_{12}N_4 \cdot 0.33H_2O$: C 73.37, H 4.58, N 20.13, found: C 73.12, H 4.89, N 20.21.

2-(4-Methylphenyl)-9-methyl-9H-imidazo[1,2-*a*]benzimidazole (11). According to method C, **8c** (0.10 g, 0.28 mmol) was dissolved in a mixture of MeOH and 1 M NaOH. Compound **11** was obtained as a white solid (0.031 g, 42%): HRMS-ESI: m/z $[M]^+$ calcd for $C_{17}H_{15}N_3$: 261.1266, found: 261.1268; Anal. calcd for $C_{17}H_{15}N_3 \cdot 0.1H_2O$: C 77.60, H 5.82, N 15.97, found: C 77.87, H 6.11, N 15.59; reference [50].

2-(4-Nitrophenyl)-9-methyl-9H-imidazo[1,2-*a*]benzimidazole (12). According to method C, **8d** (1.02 g, 2.6 mmol) was dissolved in MeOH with K_2CO_3 . Compound **12** was purified by silica column chromatography and EtOAc, and was obtained as an other solid (0.647 g, 85%): HRMS-ESI: m/z $[M]^+$ calcd for $C_{16}H_{12}N_4O_2$: 292.0960, found: 292.0959; Anal. calcd for $C_{16}H_{12}N_4O_2 \cdot 0.66H_2O$: C 63.15, H 4.42, N 18.41, found: C 63.51, H 4.31, N 18.15; reference [51].

2-(3-Nitrophenyl)-9-methyl-9H-imidazo[1,2-*a*]benzimidazole (13). According to method C, **8e** (1.64 g, 4.2 mmol) was dissolved in MeOH with K_2CO_3 . Compound **13** was purified by silica column chromatography and EtOAc, and was obtained as an other solid (0.570 g, 46%): HRMS-ESI: m/z $[M]^+$ calcd for $C_{16}H_{12}N_3O_2$: 292.0960, found: 292.0957; Anal. calcd for $C_{16}H_{12}N_3O_2$: C 65.75, H 4.14, N 19.17, found: C 65.74, H 4.24, N 18.90; reference [51].

2-(4-Methoxyphenyl)-9-methyl-9H-imidazo[1,2-*a*]benzimidazole (14). According to method C, **8g** (1.10 g, 2.9 mmol) was dissolved in a mixture of MeOH and 1 M NaOH. Compound **14** was obtained as a pale-yellow solid (0.195 g, 24%): 1H NMR (500 MHz, $[D_6]DMSO$): δ = 8.03 (s, 1H), 7.77 (d, J = 8.8 Hz, 2H), 7.71 (d, J = 7.6 Hz, 1H), 7.50 (d, J = 7.9 Hz, 1H), 7.30 (t, J = 7.3 Hz, 1H), 7.19 (t, J = 7.25 Hz, 1H),

6.95 (d, J = 8.0 Hz, 2H), 3.77 (s, 3H), 3.74 (s, 3H); ^{13}C NMR (125 MHz, $[D_6]DMSO$): δ = 158.3, 149.9, 143.4, 136.0, 127.9, 126.00 (2C), 124.1, 123.1, 120.0, 114.1 (2C), 111.1, 110.1, 101.8, 55.2, 29.14 ppm; IR (ATR): $\tilde{\nu}$ = 1599, 1487, 1442, 1419, 1299, 1242, 1172, 1125, 1063, 1030, 820, 748, 719, 687, 609, 554, 520, 435 cm^{-1} ; HRMS-ESI: m/z $[M]^+$ calcd for $C_{17}H_{15}N_3O$: 277.1215, found: 277.1216; Anal. calcd for $C_{17}H_{15}N_3O \cdot 0.2H_2O$: C 72.68, H 5.53, N 14.96, found: C 72.55, H 5.45, N 14.72.

2-(3-Methoxyphenyl)-9-methyl-9H-imidazo[1,2-*a*]benzimidazole (15). According to method C, **8f** (0.80 g, 2.1 mmol) was dissolved in a mixture of MeOH and 1 M NaOH. Compound **15** was obtained as white needles (0.215 g, 36%): 1H NMR (500 MHz, $[D_6]DMSO$): δ = 8.19 (s, 1H), 7.73 (d, J = 7.5 Hz, 1H), 7.52 (d, J = 7.9 Hz, 1H), 7.43 (m, J = 1.5 Hz, 2H), 7.30 (m, J = 1.0 Hz, 2H), 7.19 (dt, J = 7.7, 1.0 Hz, 1H), 6.80 (m, 1H), 3.81 (s, 3H), 3.75 ppm (s, 3H); ^{13}C NMR (125 MHz, $[D_6]DMSO$): δ = 159.7, 149.9, 143.2, 136.6, 136.1, 129.7, 124.0, 123.4, 120.09, 117.1, 112.50, 111.2, 110.2, 109.9, 103.4, 55.2, 29.2 ppm; IR (ATR): $\tilde{\nu}$ = 1607, 1578, 1532, 1497, 1441, 1304, 1266, 1211, 1166, 1123, 1059, 1041, 884, 819, 752, 732, 671, 630, 555 cm^{-1} ; HRMS-ESI: m/z $[M]^+$ calcd for $C_{17}H_{15}N_3O$: 277.1215, found: 277.1215; Anal. calcd for $C_{17}H_{15}N_3O$: C 73.63, H 5.45, N 15.15, found: C 73.62, H 5.51, N 15.10.

2-(2-Methoxyphenyl)-9-methyl-9H-imidazo[1,2-*a*]benzimidazole (16). According to method C, **8h** (1.56 g, 4 mmol) was dissolved in MeOH with K_2CO_3 . Compound **16** was obtained as a pale-yellow solid (1.01 g, 91%): 1H NMR (500 MHz, $[D_6]DMSO$): δ = 8.20 (dd, J = 7.7, 1.0 Hz, 1H), 8.16 (s, 1H), 7.82 (d, J = 7.9 Hz, 1H), 7.50 (d, J = 7.9 Hz, 1H), 7.31 (t, J = 8.2 Hz, 1H), 7.20 (qi, J = 7.9 Hz, 2H), 7.08 (d, J = 8.2 Hz, 1H), 7.01 (t, J = 7.3 Hz, 1H), 3.97 (s, 3H), 3.74 ppm (s, 3H); ^{13}C NMR (125 MHz, $[D_6]DMSO$): δ = 156.0, 149.1, 139.00, 136.3, 127.4, 127.3, 124.2, 123.4, 123.2, 120.5, 120.0, 111.3 (2C), 110.0, 107.00, 55.5, 29.1 ppm; IR (ATR): $\tilde{\nu}$ = 2932, 1629, 1608, 1498, 1445, 1283, 1241, 1180, 1115, 1055, 1022, 741, 695, 633, 556, 520, 429 cm^{-1} ; HRMS-ESI: m/z $[M]^+$ calcd for $C_{17}H_{15}N_3O$: 277.1215, found: 277.1216; Anal. calcd for $C_{17}H_{15}N_3O$: C 73.63, H 5.45, N 15.15, found: C 73.56, H 5.70, N 15.09.

9-Methyl-2-naphth-2-yl-9H-imidazo[1,2-*a*]benzimidazole (17). According to method C, **8i** (1.59 g, 4 mmol) was dissolved in MeOH with K_2CO_3 . Compound **17** was obtained as a pale-pink solid (0.710 g, 96%): 1H NMR (500 MHz, $[D_6]DMSO$): δ = 8.39 (s, 1H), 8.32 (s, 1H), 7.99 (d, J = 8.5 Hz, 1H), 7.95 (d, J = 8.2 Hz, 1H), 7.91 (d, J = 8.5 Hz, 1H), 7.87 (d, J = 7.9 Hz, 1H), 7.78 (d, J = 7.9 Hz, 1H), 7.54 (d, J = 7.9 Hz, 1H), 7.49 (t, J = 7.9 Hz, 1H), 7.44 (t, J = 7.3 Hz, 1H), 7.34 (t, J = 7.9 Hz, 1H), 7.22 (t, J = 7.6 Hz, 1H), 3.78 ppm (s, 3H); ^{13}C NMR (125 MHz, $[D_6]DMSO$): δ = 150.2, 143.4, 136.2, 133.6, 132.7, 132.3, 128.8, 128.00, 127.7, 126.4, 125.5, 124.0, 123.7, 123.4, 122.5, 120.2, 111.3, 110.3, 103.9, 29.2 ppm; IR (ATR): $\tilde{\nu}$ = 1712, 1627, 1497, 1126, 893, 856, 819, 733, 718, 656, 471, 430 cm^{-1} ; HRMS-ESI: m/z $[M]^+$ calcd for $C_{20}H_{15}N_3$: 297.1266, found: 297.1263; Anal. calcd for $C_{20}H_{15}N_3$: C 80.78, H 5.08, N 14.13, found: C 80.32, H 5.36, N 13.82.

2-(4-Chlorophenyl)-9-methyl-9H-imidazo[1,2-*a*]benzimidazole (18). According to method C, **8j** (0.69 g, 1.8 mmol) was dissolved in MeOH with K_2CO_3 . Compound **18** was obtained as a white solid (0.421 g, 83%): 1H NMR (500 MHz, $[D_6]DMSO$): δ = 8.19 (s, 1H), 7.85 (d, J = 8.2 Hz, 2H), 7.72 (d, J = 7.9 Hz, 1H), 7.50 (d, J = 8.2 Hz, 1H), 7.42 (d, J = 8.2 Hz, 2H), 7.32 (t, J = 7.8 Hz, 1H), 7.19 (t, J = 7.8 Hz, 1H), 3.73 ppm (s, 3H); ^{13}C NMR (125 MHz, $[D_6]DMSO$): δ = 150.0, 142.1, 136.1, 134.1, 130.9, 128.7 (2C), 126.3 (2C), 123.9, 123.5, 120.1, 111.3, 110.2, 103.6, 29.1 ppm; IR (ATR): $\tilde{\nu}$ = 1704, 1589, 1438, 1125, 1086, 1008, 827, 738, 721, 683, 566, 529, 498, 430 cm^{-1} ; HRMS-ESI: m/z $[M]^+$ calcd for $C_{16}H_{12}ClN_3$: 281.0720, found:

281.0717; Anal. calcd for $C_{16}H_{12}ClN_3 \cdot 0.1H_2O$: C 67.78, H 4.34, N 14.82, found: C 67.74, H 4.43, N 14.57.

2-(4-Aminophenyl)-9-methyl-9H-imidazo[1,2-a]benzimidazole

(19). A solution of **12** (0.29 g, 1.0 mmol) in 100 mL MeOH was treated with H_2 and Pd/C (10%) and stirred at room temperature under pressure (4 bar) for 12 h. The catalyst was removed, the solvent was concentrated, and the residue was treated with H_2O . Compound **19** was obtained as a pale-yellow solid (0.100 g, 37%): 1H NMR (500 MHz, $[D_6]DMSO$): δ = 7.84 (s, 1H), 7.67 (d, J = 7.6 Hz, 1H), 7.53 (d, J = 8.5 Hz, 2H), 7.47 (d, J = 7.9 Hz, 1H), 7.27 (dt, J = 8.1, 1.3 Hz, 1H), 7.16 (dt, J = 7.7, 1.3 Hz, 1H), 6.59 (d, J = 8.5 Hz, 2H), 5.09 (s, 2H), 3.72 ppm (s, 3H); ^{13}C NMR (125 MHz, $[D_6]DMSO$): δ = 149.8, 147.8, 144.7, 135.9, 125.7 (2C), 124.2, 130.2, 122.8, 119.9, 114.1 (2C), 110.8, 110.0, 100.2, 29.1 ppm; IR (ATR): $\tilde{\nu}$ = 1598, 1492, 1287, 1177, 1125, 1060, 832, 740, 611, 516 cm^{-1} ; HRMS-ESI: m/z $[M]^+$ calcd for $C_{16}H_{14}N_4$: 262.1218, found: 262.1220; Anal. calcd for $C_{16}H_{12}ClN_3 \cdot 0.25H_2O$: C 72.02, H 5.48, N 21.00, found: C 72.19, H 5.49, N 20.65.

2-(3-Aminophenyl)-9-methyl-9H-imidazo[1,2-a]benzimidazole

(20). A solution of **13** (0.29 g, 1.0 mmol) in 100 mL MeOH was treated with H_2 and Pd/C (10%) and stirred at room temperature under pressure (4 bar) for 12 h. The catalyst was removed, the solvent was concentrated, and the residue was treated with H_2O . Compound **20** was obtained as a pale-yellow solid (0.230 g, 80%): 1H NMR (500 MHz, $[D_6]DMSO$): δ = 8.00 (s, 1H), 7.72–7.75 (m, 1H), 7.50 (d, 1H, J = 7.9 Hz), 7.28–7.32 (m, 1H), 7.16–7.20 (m, 2H), 6.98–7.03 (m, 2H), 6.44–6.46 (m, 1H), 5.03 (s, 2H), 3.73 ppm (s, 3H); ^{13}C NMR (125 MHz, $[D_6]DMSO$): δ = 149.8, 148.9, 144.2, 136.1, 135.6, 129.0, 124.1, 123.18, 120.00, 112.7 (2C), 111.2, 110.7, 110.1, 102.6, 29.1 ppm; IR (ATR): $\tilde{\nu}$ = 3052, 1603, 1536, 1491, 1450, 1308, 1272, 1232, 1188, 1124, 1063, 779, 739, 705, 645, 553, 431 cm^{-1} ; HRMS-ESI: m/z $[M]^+$ calcd for $C_{16}H_{14}N_4$: 262.1218, found: 262.1220; Anal. calcd for $C_{16}H_{12}ClN_3 \cdot 1.1H_2O$: C 68.12, H 5.79, N 19.86, found: C 67.87, H 6.19, N 19.59.

4-(9-Benzyl-9H-imidazo[1,2-a]benzimidaz-2-yl)benzonitrile

(21). According to method C, **8k** (0.10 g, 0.22 mmol) was dissolved in a solution of K_2CO_3 in MeOH. Compound **21** was obtained as white needles (0.062 g, 75%): 1H NMR (125 MHz, $[D_6]DMSO$): δ = 8.45 (s, 1H), 8.02 (d, J = 8.3 Hz, 2H), 7.82 (d, J = 8.3 Hz, 2H), 7.78 (d, J = 7.8 Hz, 1H), 7.56 (d, J = 8.1 Hz, 1H), 7.41 (d, J = 7.4 Hz, 2H), 7.29–7.34 (m, 3H), 7.20–7.28 (m, 2H), 5.45 ppm (s, 2H); ^{13}C NMR (125 MHz, $[D_6]DMSO$): δ = 149.9, 141.6, 139.7, 136.7, 135.4, 132.7 (2C), 128.8 (2C), 127.9, 127.6 (2C), 125.2 (2C), 124.0, 123.9, 120.7, 119.3, 111.8, 110.9, 108.6, 105.9, 46.1 ppm; IR (ATR): $\tilde{\nu}$ = 2222, 1607, 1495, 1425, 1344, 1199, 1130, 1058, 837, 744, 702, 681, 544, 433 cm^{-1} ; HRMS-ESI: m/z $[M]^+$ calcd for $C_{23}H_{16}N_4$: 348.1375, found: 348.1373; Anal. calcd for $C_{23}H_{16}N_4 \cdot 0.6H_2O$: C 76.90, H 4.83, N 15.60, found: C 77.18, H 4.65, N 15.22.

9-Benzyl-2-(4-methylphenyl)-9H-imidazo[1,2-a]benzimidazole

(22). According to method C, **8l** (0.50 g, 1.12 mmol) was dissolved in a mixture of MeOH and 1 M NaOH. Compound **22** was obtained as a white solid (0.285 g, 42%): 1H NMR (125 MHz, $[D_6]DMSO$): δ = 7.86 (s, 1H), 7.74 (d, 2H, J = 8.1 Hz), 7.68 (d, 1H, J = 7.5 Hz), 7.37 (d, 2H, J = 7.5 Hz), 7.29–7.35 (m, 3H), 7.24–7.29 (m, 3H), 7.18–7.24 (m, 3H), 5.48 (s, 2H), 4.89 (s, 2H), 2.36 ppm (s, 3H); ^{13}C NMR (125 MHz, $[D_6]DMSO$): δ = 151.5, 145.7, 138.3, 138.0, 136.9, 133.4, 130.5 (2C), 130.1 (2C), 129.2, 128.5 (2C), 126.5 (2C), 126.2, 124.9, 122.2, 112.5, 112.0, 103.6, 47.8, 21.54 ppm; IR (ATR): $\tilde{\nu}$ = 1601, 1495, 1430, 1311, 1197, 1128, 1061, 819, 731, 705, 680, 637, 556, 503, 457, 431 cm^{-1} ; HRMS-ESI: m/z $[M]^+$ calcd for $C_{23}H_{19}N_3$: 337.1579, found: 337.1575;

Anal. calcd for $C_{23}H_{19}N_3 \cdot 0.2H_2O$: C 81.01, H 5.73, N 12.12, found: C 80.92, H 5.92, N 12.32.

9-Benzyl-2-(4-nitrophenyl)-9H-imidazo[1,2-a]benzimidazole (23).

According to method C, **8m** (0.33 g, 0.7 mmol) was dissolved in a solution of K_2CO_3 in MeOH. Compound **23** was purified by silica column chromatography and EtOAc, and was obtained as a yellow solid (0.253 g, 67%): 1H NMR (125 MHz, $[D_6]DMSO$): δ = 8.53 (s, 1H), 8.22 (d, J = 8.8 Hz, 2H), 8.09 (d, J = 8.8 Hz, 2H), 7.80 (d, J = 7.9 Hz, 1H), 7.57 (d, J = 8.0 Hz, 1H), 7.42 (d, J = 7.4 Hz, 2H), 7.29–7.35 (m, 3H), 7.20–7.29 (m, 2H), 5.46 ppm (s, 2H); ^{13}C NMR (125 MHz, $[D_6]DMSO$): δ = 150.0, 145.6, 141.8, 141.3, 136.7, 135.5, 128.5 (2C), 127.9, 127.5 (2C), 125.2 (2C), 124.3 (2C), 124.1, 123.9, 120.7, 111.9, 110.9, 106.7, 46.1 ppm; IR (ATR): $\tilde{\nu}$ = 1608, 1495, 1431, 1334, 1201, 1106, 844, 738, 704, 431 cm^{-1} ; HRMS-ESI: m/z $[M]^+$ calcd for $C_{22}H_{16}N_4O_2$: 368.1273, found: 368.1271; Anal. calcd for $C_{23}H_{19}N_3 \cdot 0.5H_2O$: C 70.02, H 4.54, N 14.85, found: C 70.32, H 4.60, N 13.97.

9-Benzyl-2-(4-methoxyphenyl)-9H-imidazo[1,2-a]benzimidazole

(24). According to methods B and C, 1-benzylbenzimidazole-2-amine (0.050 g, 0.25 mmol) and 2-bromo-4'-methoxyacetophenone (0.075 g, 0.3 mmol) were first reacted in acetone and subsequently in MeOH with K_2CO_3 . Compound **24** was obtained as a white solid (0.054 g, 67%): 1H NMR (125 MHz, $[D_6]DMSO$): δ = 8.07 (s, 1H), 7.78 (d, J = 8.8 Hz, 2H), 7.73 (d, J = 7.7 Hz, 1H), 7.52 (d, J = 8.0 Hz, 1H), 7.40 (d, J = 7.3 Hz, 2H), 7.31 (t, J = 7.4 Hz, 2H), 7.23–7.28 (m, 1H), 7.19 (dt, J = 7.8, 0.9 Hz, 1H), 6.96 (d, J = 8.8 Hz, 2H), 5.44 (s, 2H), 3.77 ppm (s, 3H); ^{13}C NMR (125 MHz, $[D_6]DMSO$): δ = 158.4; 149.5, 143.5, 136.9, 135.1, 128.8 (2C), 127.8, 127.5 (2C), 126.0 (2C), 124.2, 123.2, 120.4, 114.1 (2C), 111.3, 110.6, 102.0, 55.2, 46.0 ppm; IR (ATR): $\tilde{\nu}$ = 1602, 1487, 1430, 1235, 1172, 1061, 1028, 831, 737, 687, 588, 556, 454, 430 cm^{-1} ; HRMS-ESI: m/z $[M]^+$ calcd for $C_{23}H_{19}N_3O$: 353.1528, found: 353.1524; Anal. calcd for $C_{23}H_{19}N_3O \cdot 0.5H_2O$: C 76.22, H 5.56, N 11.59, found: C 76.03, H 5.26, N 11.54.

4-(9-(2-Methylallyl)-9H-imidazo[1,2-a]benzimidaz-2-yl)benzonitrile

(25). According to methods B and C, **7b** (0.19 g, 1.0 mmol) and 2-bromo-4'-cyanoacetophenone (0.25 g, 1.1 mmol) were first reacted in acetone and subsequently in MeOH with K_2CO_3 . Compound **25** was obtained as a white solid (0.217 g, 65%): 1H NMR (125 MHz, $[D_6]DMSO$): δ = 8.43 (s, 1H), 8.01 (d, J = 8.4 Hz, 2H), 7.81 (d, J = 8.5 Hz, 2H), 7.78 (d, J = 7.9 Hz, 1H), 7.47 (d, J = 8.1 Hz, 1H), 7.32 (dt, J = 7.8, 1.1 Hz, 1H), 7.23 (dt, J = 7.9, 0.9 Hz, 1H), 4.92 (s, 1H), 4.78 (s, 2H), 4.74 (s, 1H), 1.72 ppm (s, 3H, CH_3); ^{13}C NMR (125 MHz, $[D_6]DMSO$): δ = 149.6, 141.6, 139.8, 139.7, 135.7, 132.7 (2C), 125.1 (2C), 123.9, 123.8, 120.5, 119.4, 112.3, 111.7, 110.9, 108.5, 105.8, 48.3, 19.9 ppm; IR (ATR): $\tilde{\nu}$ = 3270, 2217, 1608, 1496, 1444, 1265, 1201, 1128, 1062, 889, 841, 744, 693, 547, 430 cm^{-1} ; HRMS-ESI: m/z $[M]^+$ calcd for $C_{20}H_{16}N_4$: 312.1375, found: 312.1373; Anal. calcd for $C_{23}H_{19}N_3O \cdot 1.25H_2O$: C 71.73, H 5.57, N 16.73, found: C 71.75, H 5.36, N 16.50.

4-(9-(4-Methoxybenzyl)-9H-imidazo[1,2-a]benzimidaz-2-yl)benzonitrile

(26). According to methods B and C, **7d** (0.25 g, 1.0 mmol) and 2-bromo-4'-cyanoacetophenone (0.25 g, 1.1 mmol) were first reacted in acetone and subsequently in MeOH with K_2CO_3 . Compound **26** was purified by silica column chromatography and EtOAc, and was obtained as a white solid (0.200 g, 52%): 1H NMR (125 MHz, $[D_6]DMSO$): δ = 8.45 (s, 1H), 8.04 (d, J = 8.5 Hz, 2H), 7.84 (d, J = 7.5 Hz, 2H), 7.78 (d, J = 7.5 Hz, 1H), 7.60 (d, J = 8.1 Hz, 1H), 7.39 (d, J = 8.7 Hz, 2H), 7.32 (dt, J = 8.1, 1.1 Hz, 1H), 7.22 (dt, J = 7.7, 1.0 Hz, 1H), 6.88 (d, J = 8.8 Hz, 2H), 5.38 (s, 2H), 3.69 ppm (s, 3H); ^{13}C NMR (125 MHz, $[D_6]DMSO$): δ = 159.0, 149.9, 141.6, 139.7, 135.3, 132.7 (2C), 129.1 (2C), 128.7, 125.1 (2C), 124.0,

123.9, 120.6, 119.4, 114.2 (2C), 111.8, 110.9, 108.6, 105.9, 55.2, 45.6 ppm; IR (ATR): $\tilde{\nu}$ = 3151, 2223, 1607, 1513, 1495, 1431, 1294, 1244, 1174, 1060, 1029, 856, 837, 801, 737, 704, 545, 508, 429 cm^{-1} ; HRMS-ESI: m/z $[M]^+$ calcd for $\text{C}_{24}\text{H}_{18}\text{N}_4\text{O}$: 378.1481, found: 378.1478; Anal. calcd for $\text{C}_{24}\text{H}_{18}\text{N}_4\text{O} \cdot 0.33\text{H}_2\text{O}$: C 74.98, H 4.89, N 14.57, found: C 74.73, H 5.30, N 14.45.

4-(9-(3,4-Difluorobenzyl)-9H-imidazo[1,2-a]benzimidaz-2-yl)benzotriazole (27). According to methods B and C, **7e** (0.26 g, 1.0 mmol) and 2-bromo-4'-cyanoacetophenone (0.26 g, 1.2 mmol) were first reacted in acetone and subsequently in MeOH with K_2CO_3 . Compound **27** was purified by silica column chromatography and EtOAc, and was obtained as a white solid (0.200 g, 52%): ^1H NMR (125 MHz, $[\text{D}_6]\text{DMSO}$): δ = 8.46 (s, 1H), 8.02 (d, J = 8.5 Hz, 2H), 7.82 (d, J = 8.3 Hz, 2H), 7.79 (d, J = 7.9 Hz, 1H), 7.61 (d, J = 8.1 Hz, 1H), 7.52–7.57 (m, 1H), 7.34–7.41 (m, 1H), 7.33 (dt, J = 8.1, 1.1 Hz, 1H), 7.22–7.27 (m, 2H), 5.45 ppm (s, 2H); ^{13}C NMR (125 MHz, $[\text{D}_6]\text{DMSO}$): δ = 150.3 (dd, J = 42.7, 12.6 Hz), 149.7, 148.3 (dd, J = 42.0, 12.6 Hz), 141.6, 139.6, 135.3, 134.4 (dd, J = 5.1, 4.0 Hz), 132.8 (2C), 125.1 (2C), 124.5 (dd, J = 6.6, 3.4 Hz), 124.1, 124.0, 120.8, 119.3, 118.0 (d, J = 17.2 Hz), 116.9 (d, J = 17.5 Hz), 111.9, 110.8, 108.6, 106.1, 45.1 ppm; IR (ATR): $\tilde{\nu}$ = 2221, 1609, 1518, 1494, 1432, 1276, 1200, 1112, 1061, 842, 802, 780, 738, 683, 645, 546, 513, 428 cm^{-1} ; HRMS-ESI: m/z $[M]^+$ calcd for $\text{C}_{23}\text{H}_{14}\text{F}_2\text{N}_4$: 384.1187, found: 384.1185; Anal. calcd for $\text{C}_{23}\text{H}_{14}\text{F}_2\text{N}_4 \cdot 0.2\text{H}_2\text{O}$: C 71.20, H 3.74, N 14.44, found: C 71.41, H 4.00, N 14.15.

4-(9-(3,4-Dichlorobenzyl)-9H-imidazo[1,2-a]benzimidaz-2-yl)benzotriazole (28). According to methods B and C, **7f** (0.29 g, 1.0 mmol) and 2-bromo-4'-cyanoacetophenone (0.25 g, 1.1 mmol) were first reacted in acetone and subsequently in MeOH with K_2CO_3 . Compound **28** was obtained as a white solid (0.272 g, 64%): ^1H NMR (125 MHz, $[\text{D}_6]\text{DMSO}$): δ = 8.45 (s, 1H), 8.01 (d, J = 8.6 Hz, 2H), 7.81 (d, J = 8.6 Hz, 2H), 7.78 (dd, J = 8.0, 0.6 Hz, 1H), 7.74 (d, J = 2.1 Hz, 1H), 7.60 (d, J = 8.0 Hz, 1H), 7.57 (d, J = 8.3 Hz, 1H), 7.31–7.38 (m, 2H), 7.23 (dt, J = 7.7, 1.0 Hz, 1H), 5.46 ppm (s, 2H); ^{13}C NMR (125 MHz, $[\text{D}_6]\text{DMSO}$): δ = 149.7, 141.6, 139.6, 137.8, 135.3, 132.7 (2C), 131.4, 131.1, 130.6, 129.7, 127.8, 125.1 (2C), 124.1, 124.0, 120.9, 119.3, 111.9, 110.8, 108.6, 106.1, 44.9 ppm; IR (ATR): $\tilde{\nu}$ = 2221, 1624, 1609, 1497, 1432, 1264, 1202, 1128, 1060, 1031, 880, 849, 823, 737, 677, 639, 547, 468, 429 cm^{-1} ; HRMS-ESI: m/z $[M]^+$ calcd for $\text{C}_{23}\text{H}_{14}\text{Cl}_2\text{N}_4$: 416.0596, found: 416.0595; Anal. calcd for $\text{C}_{23}\text{H}_{14}\text{Cl}_2\text{N}_4$: C 66.20, H 3.38, N 13.43, found: C 65.81, H 3.34, N 13.09.

4-(9-((6-chloro-4H-benzo[1,3]dioxin-8-yl)methyl)-9H-imidazo[1,2-a]benzimidaz-2-yl)benzotriazole (29). According to methods B and C, **7h** (0.32 g, 1.0 mmol) and 2-bromo-4'-cyanoacetophenone (0.25 g, 1.1 mmol) were first reacted in acetone in MeOH with K_2CO_3 . Compound **29** was obtained as a white solid (0.360 g, 82%): ^1H NMR (125 MHz, $[\text{D}_6]\text{DMSO}$): δ = 8.45 (s, 1H), 8.00 (d, J = 8.5 Hz, 2H), 7.78–7.83 (m, 3H), 7.49 (d, J = 8.1 Hz, 1H), 7.33 (dt, J = 7.9, 0.9 Hz, 1H), 7.24 (dt, J = 7.9, 0.9 Hz, 1H), 7.12 (d, J = 2.5 Hz, 1H), 7.00 (d, J = 2.5 Hz, 1H), 5.35 (s, 4H), 4.88 ppm (s, 2H); ^{13}C NMR (125 MHz, $[\text{D}_6]\text{DMSO}$): δ = 149.7, 148.9, 141.6, 139.6, 135.5, 132.7 (2C), 129.3, 125.8, 125.1 (2C), 125.0, 124.6, 124.1, 124.0, 123.9, 120.8, 119.3, 110.8 (2C), 108.6, 106.1, 91.4, 65.3, 40.4 ppm; IR (ATR): $\tilde{\nu}$ = 2216, 1626, 1609, 1494, 1444, 1341, 1220, 1196, 1128, 1082, 1062, 985, 951, 865, 846, 730, 694, 644, 547, 432 cm^{-1} ; HRMS-ESI: m/z $[M]^+$ calcd for $\text{C}_{25}\text{H}_{17}\text{ClN}_4\text{O}_2$: 440.1040, found: 440.1039; Anal. calcd for $\text{C}_{25}\text{H}_{17}\text{ClN}_4\text{O}_2$: C 68.11, H 3.89, N 12.71, found: C 67.68, H 4.01, N 12.61.

4-(9-(Phenylethyl)-9H-imidazo[1,2-a]benzimidaz-2-yl)benzotriazole (30). According to methods B and C, **7a** (0.20 g, 1.0 mmol) and 2-

bromo-4'-cyanoacetophenone (0.25 g, 1.1 mmol) were first reacted in acetone and subsequently in MeOH with K_2CO_3 . Compound **30** was obtained as a white solid (0.293 g, 94%): ^1H NMR (125 MHz, $[\text{D}_6]\text{DMSO}$): δ = 8.40 (s, 1H), 8.02 (d, J = 8.3 Hz, 2H), 7.82 (d, J = 8.3 Hz, 2H), 7.74 (d, J = 7.8 Hz, 1H), 7.45 (d, J = 8.1 Hz, 1H), 7.19–7.29 (m, 6H), 7.12–7.16 (m, 1H), 4.45 (t, J = 7.3 Hz, 2H), 3.22 ppm (t, J = 7.3 Hz, 2H); ^{13}C NMR (125 MHz, $[\text{D}_6]\text{DMSO}$): δ = 149.7, 141.6, 139.8, 138.3, 135.7, 132.7 (2C), 128.9 (2C), 128.5 (2C), 126.5, 125.2 (2C), 123.8, 123.7, 120.2, 119.4, 111.6, 110.6, 108.5, 105.6, 44.3, 33.7 ppm; IR (ATR): $\tilde{\nu}$ = 2219, 1606, 1493, 1429, 1192, 1129, 1059, 844, 739, 693, 548, 498, 427 cm^{-1} ; HRMS-ESI: m/z $[M]^+$ calcd for $\text{C}_{24}\text{H}_{18}\text{N}_4$: 362.1531, found: 362.1532; Anal. calcd for $\text{C}_{25}\text{H}_{17}\text{ClN}_4\text{O}_2 \cdot 0.5\text{H}_2\text{O}$: C 77.61, H 5.16, N 15.08, found: C 77.40, H 4.93, N 14.75.

4-(9-(3-Phenylpropyl)-9H-imidazo[1,2-a]benzimidaz-2-yl)benzotriazole (31). According to methods B and C, **7c** (0.094 g, 1.0 mmol) and 2-bromo-4'-cyanoacetophenone (0.25 g, 1.1 mmol) were first reacted in acetone and subsequently in MeOH with K_2CO_3 . Compound **31** was obtained as a white solid (0.025 g, 2%): ^1H NMR (125 MHz, $[\text{D}_6]\text{DMSO}$): δ = 8.42 (s, 1H), 8.02 (d, J = 8.3 Hz, 2H), 7.82 (d, J = 8.3 Hz, 2H), 7.77 (d, J = 7.8 Hz, 1H), 7.53 (d, J = 8.1 Hz, 1H), 7.34 (t, J = 7.7 Hz, 1H), 7.19–7.28 (m, 5H), 7.16 (t, J = 7.0 Hz, 1H), 4.25 (t, J = 7.0 Hz, 2H), 2.68 (t, J = 8.0 Hz, 2H), 2.21 ppm (qi, J = 7.5 Hz, 2H); ^{13}C NMR (125 MHz, $[\text{D}_6]\text{DMSO}$): δ = 149.9, 141.6, 141.2, 135.7, 139.8, 132.8 (2C), 128.4 (2C), 128.4 (2C), 126.0, 125.1, 123.9, 123.8, 120.3, 119.4, 111.7, 110.5, 108.5, 105.7, 42.6, 32.42, 29.6 ppm; IR (ATR): $\tilde{\nu}$ = 2228, 1604, 1491, 1425, 1356, 1061, 836, 742, 693, 545, 491, 425 cm^{-1} ; HRMS-ESI: m/z $[M]^+$ calcd for $\text{C}_{25}\text{H}_{20}\text{N}_4$: 376.1688, found: 376.1686; Anal. calcd for $\text{C}_{25}\text{H}_{20}\text{N}_4 \cdot 1.0\text{H}_2\text{O}$: C 76.12, H 5.62, N 14.20, found: C 76.37, H 5.24, N 14.16.

4-(9-(2-(Piperidin-1-yl)ethyl)-9H-imidazo[1,2-a]benzimidaz-2-yl)benzotriazole (32). According to methods B and C, **7g** (0.22 g, 0.9 mmol) and 2-bromo-4'-cyanoacetophenone (0.25 g, 1.1 mmol) were first reacted in acetone and subsequently in MeOH with K_2CO_3 . Compound **32** was obtained as a white solid (0.220 g, 65%): ^1H NMR (125 MHz, $[\text{D}_6]\text{DMSO}$): δ = 8.39 (s, 1H), 8.00 (d, J = 8.5 Hz, 1H), 7.81 (d, J = 8.6 Hz, 2H), 7.75 (d, J = 7.6 Hz, 1H), 7.57 (d, J = 8.1 Hz, 1H), 7.33 (dt, J = 8.0, 1.1 Hz, 1H), 7.20 (dt, J = 8.0, 1.1 Hz, 1H), 4.30 (t, J = 6.5 Hz, 2H), 2.73 (t, J = 6.5 Hz, 2H), 2.36–2.44 (m, 4H), 1.32–1.38 (m, 4H), 1.27–1.32 ppm (m, 2H); ^{13}C NMR (125 MHz, $[\text{D}_6]\text{DMSO}$): δ = 150.0, 141.6, 139.8, 136.0, 132.8 (2C), 125.1 (2C), 123.9, 123.8, 120.3, 119.5, 111.6, 110.8, 108.5, 105.6, 56.2, 54.2 (2C), 40.7, 25.7 (2C), 24.1 ppm; IR (ATR): $\tilde{\nu}$ = 2934, 2217, 1608, 1494, 1433, 1261, 1192, 1127, 1060, 842, 736, 682, 639, 548, 429 cm^{-1} ; HRMS-ESI: m/z $[M]^+$ calcd for $\text{C}_{23}\text{H}_{23}\text{N}_5$: 369.1953, found: 369.1945; Anal. calcd for $\text{C}_{23}\text{H}_{23}\text{N}_5 \cdot 0.5\text{H}_2\text{O}$: C 72.99, H 6.39, N 18.50, found: C 72.64, H 6.10, N 18.18.

Reagents for biological investigation

Daunorubicin-HCl, vinblastine sulfate, and rhodamine 123 were obtained from Fluka; 3-(4,5-dimethylthiazole-2-yl)-2,5-diphenyltetrazolium bromide was purchased from AppliChem. Antibodies were obtained from BD Pharmingen (FITC-labeled 17F9 anti-P-gp), Signet Laboratories (C219), and Calbiochem (horseradish peroxidase (HRP)-conjugated anti-mouse IgG). All other chemicals, unless otherwise stated, were obtained from Sigma. Stock solutions (10 mM) of tested compounds were prepared in DMSO. XR9576 was synthesized according to Roe et al.^[54]

Cell lines

The human ovarian cancer cell lines A2780 and A2780 Adr were obtained from the European Collection of Cell Cultures (ECACC, UK, Nos. 93112519 and 93112520, respectively) and cultured in RPMI 1640 medium (Sigma) supplemented with 10% fetal bovine serum and 50 $\mu\text{g mL}^{-1}$ penicillin and streptomycin at 37 °C in a humidified atmosphere containing 5% CO_2 . Every ten passages P-gp-overexpressing A2780 Adr cells were treated with 1 μM doxorubicin to maintain high levels of P-gp expression.

Preparation of crude cell membranes

Cells were grown to a confluency of ~90% in TC dishes, harvested, and resuspended in cold HEPES buffer (20 mM, pH 7.4) with Na_2EDTA (10 mM). All following steps were performed at 4 °C: After cells were destroyed by homogenization (Polytron), remaining whole cells and nuclei were separated by centrifugation (800 g, 10 min, 4 °C). The supernatant was centrifuged again (40000 g, 30 min, 2 °C), and the pellet obtained was resuspended in HEPES buffer (20 mM, pH 7.4) containing Na_2EDTA (10 mM). This step was repeated twice, and the suspension obtained was stored at -80 °C and used for Western blot analysis of P-gp expression. The total amount of protein in the samples was determined by using the Lowry method as modified by Peterson.^[55]

Western blot

Proteins from crude membranes of A2780 and A2780 Adr cells (5 μg protein per lane) were separated on a 7.5% SDS-polyacrylamide gel. The bands were blotted onto polyvinylidene difluoride membranes, and P-gp was stained with the primary mouse monoclonal anti-P-gp antibody C219 (1:640 dilution). In a second step, membranes were incubated with an HRP-conjugated anti-mouse IgG (1:20000 dilution), and stained proteins were visualized with the Immobilon Western chemiluminescent HRP substrate (Millipore).

P-gp antibody staining

P-gp expression in A2780 Adr cells was additionally monitored with the FITC-labeled anti-P-gp antibody 17F9. Cells were harvested and suspended in cold PBS containing 0.5% BSA, centrifuged (266 g, 4 min, 4 °C), and resuspended in cold PBS containing 0.5% BSA and 0.1% NaN_3 . The cells were washed twice with cold buffer, the pellet was resuspended again and 20 μL of the labeled antibody were added. After an incubation period of 40 min, cells were centrifuged, washed again, and the samples were measured using the FL-1 channel (530 \pm 30 nm) of a Becton Dickinson FACScalibur instrument equipped with an Ar laser (λ = 488 nm).

Drug accumulation assays

The intracellular accumulation of various P-gp substrates was determined with a flow-cytometry-based assay.^[25] For this purpose cells were grown to a confluency of ~90%, harvested by trypsin treatment, resuspended in Krebs-HEPES buffer, and seeded into 96-well microplates at a final density of 10⁶ cells mL⁻¹. After pre-incubation for 15 min with various concentrations (10 nM–0.1 mM) of the tested compounds, DNR (3 μM) or rho 123 (0.3 μM) was added. The intracellular fluorescence was measured after 180 min (DNR) or 120 min (rho 123) using a Becton Dickinson FACScalibur instrument

equipped with an Ar laser (λ = 488 nm). For data analysis, single living cells were gated based on the FSC versus SSC dot plot, and geometric mean values of FL-1 and FL-3, respectively, were plotted versus the logarithm of the modulator's concentration. EC₅₀ values were calculated from concentration–response curves obtained by nonlinear regression using the four-parameter logistic equation with variable slope (Prism v. 5.01, GraphPad Software Inc., La Jolla, CA, USA).

MTT assays

Determination of the toxicity of various cytotoxic drugs in the presence or absence of modulators was performed as described previously.^[56] The cytotoxic drugs vinblastine and colchicine were combined with selected nontoxic concentrations of the modulators. The degree of resistance was defined as $F_r = (IC_{50\text{resistant}}) / (IC_{50\text{sensitive}})$.

Purification of P-glycoprotein

Purification and reconstitution of P-gp from the human P-gp-expressing *S. cerevisiae* strain BJ5457 MDR1 was performed as described.^[57] Briefly, the yeast plasma membrane was isolated after mechanical cell disruption by differential centrifugation steps. After solubilization with 1% lysophosphatidylcholine and Ni-NTA affinity chromatography, the purified protein was reconstituted into a defined lipid environment via dialysis.

ATPase activity assays

The protocol for measuring the ATPase activity of purified P-gp is based on the colorimetric determination of inorganic phosphate (P_i) released by the hydrolysis of ATP, and was carried out as described previously.^[57] The reaction volume of 250 μL contained 0.9 μg purified protein. Samples (50 μL) were taken at distinct time points (0, 20, 40, and 60 min). All experiments were performed at least in duplicate using the same lot of purified P-gp to avoid potential effects from lot-to-lot variation. K_M values were calculated using the Michaelis–Menten equation. GraphPad Prism v. 5.0 was used for data fitting.

Acknowledgements

The authors thank Dr. Buko Lindner and Brigitte Kunz at the Borstel Research Center, Borstel (Germany) for performing the mass spectrometric analyses.

Keywords: activators • cooperative effects • heterocycles • MDR transporters • P-glycoprotein

- [1] A. H. Schinkel, *Semin. Cancer Biol.* **1997**, *8*, 161–170.
- [2] B. Sarkadi, L. Homolya, G. Szakacs, A. Varadi, *Physiol. Rev.* **2006**, *86*, 1179–1236.
- [3] S. Choudhuri, C. D. Klaassen, *Int. J. Toxicol.* **2006**, *25*, 231–259.
- [4] A. B. Shapiro, V. Ling, *Eur. J. Biochem.* **1997**, *250*, 130–137.
- [5] C. Martin, G. Berridge, C. F. Higgins, P. Mistry, P. Charlton, R. Callaghan, *Mol. Pharmacol.* **2000**, *58*, 624–632.
- [6] A. R. Safa, *Curr. Med. Chem. Anticancer Agents* **2004**, *4*, 1–17.
- [7] A. B. Shapiro, K. Fox, P. Lam, V. Ling, *Eur. J. Biochem.* **1999**, *259*, 841–850.
- [8] M. Wiese, I. K. Pajeva, *Curr. Med. Chem.* **2001**, *8*, 685–713.
- [9] S. Shukla, C. Wu, S. V. Ambudkar, *Expert Opin. Drug Metab. Toxicol.* **2008**, *4*, 205–223.

- [10] J. Robert, C. Jarry, *J. Med. Chem.* **2003**, *46*, 4805–4817.
- [11] G. Szakacs, J. K. Paterson, J. A. Ludwig, C. Booth-Genthe, M. M. Gottesmann, *Nat. Rev. Drug Discovery* **2006**, *5*, 219–234.
- [12] E. Wang, M. Barecki-Roach, W. W. Johnson, *Biochem. Biophys. Res. Commun.* **2002**, *297*, 412–418.
- [13] F. J. Sharom, X. Yu, G. DiDiodato, J. W. K. Chu, *Biochem. J.* **1996**, *320*, 421–428.
- [14] R. V. Kondratov, P. G. Komarov, Y. Becker, A. Ewenson, A. V. Gudkov, *Proc. Natl. Acad. Sci. USA* **2001**, *98*, 14078–14083.
- [15] X. Zhu, Q. S. Yu, R. G. Cutler, C. W. Culmsee, H. W. Holloway, D. K. Lahiri, M. P. Mattson, N. H. Greig, *J. Med. Chem.* **2002**, *45*, 5090–5097.
- [16] S. D. Barchéchath, R. I. Tawatao, M. Corr, D. A. Carson, H. B. Cottam, *J. Med. Chem.* **2005**, *48*, 6409–6422.
- [17] V. A. Ansimova, A. A. Spasov, A. F. Kucheryavenko, T. I. Panchenko, O. V. Ostrovskii, V. A. Kosolapov, N. P. Larionov, *Pharm. Chem. J.* **2002**, *36*, 528–534.
- [18] T. Mase, H. Arima, K. Tomioka, T. Yamada, K. Murase, *J. Med. Chem.* **1986**, *29*, 386–394.
- [19] V. I. Ognyanov, C. Balan, A. W. Bannon, Y. Bo, C. Dominguez, C. Fotsch, V. K. Gore, L. Klionsky, V. V. Ma, Y. Qian, R. Tamir, X. Wang, N. Xi, S. Xu, D. Zhu, N. R. Gavva, J. J. S. Treanor, M. H. Norman, *J. Med. Chem.* **2006**, *49*, 3719–3742.
- [20] T. C. Hamilton, R. C. Young, R. F. Ozols, *Semin. Oncol.* **1984**, *11*, 285–298.
- [21] E. C. Spoelstra, H. Dekker, G. J. Schuurhuis, H. J. Broxterman, J. Lankelma, *Biochem. Pharmacol.* **1991**, *41*, 349–359.
- [22] E. Okochi, T. Iwahashi, T. Tsuruo, *Leukemia* **1997**, *11*, 1119–1123.
- [23] M. Aihara, Y. Aihara, G. Schmidt-Wolf, I. Schmidt-Wolf, I. S. Branimir, K. Blume, N. J. Chao, *Blood* **1991**, *77*, 2079–2084.
- [24] H. Müller, W. Klinkhammer, C. Globisch, M. U. Kassack, I. K. Pajeva, M. Wiese, *Bioorg. Med. Chem.* **2007**, *15*, 7470–7479.
- [25] V. Jekerle, W. Klinkhammer, D. A. Scollard, K. Breitbach, R. M. Reilly, M. Piquette-Miller, M. Wiese, *Int. J. Cancer* **2006**, *119*, 414–422.
- [26] V. Jekerle, W. Klinkhammer, R. M. Reilly, M. Piquette-Miller, M. Wiese, *Cancer Chemother. Pharmacol.* **2007**, *59*, 61–69.
- [27] H. Minderman, A. Suvannasankha, K. L. O'Loughlin, G. L. Scheffer, R. J. Scheper, R. W. Robey, M. R. Baer, *Cytometry* **2002**, *48*, 59–65.
- [28] A. Pick, H. Müller, M. Wiese, *Bioorg. Med. Chem.* **2008**, *16*, 8224–8236.
- [29] I. K. Pajeva, C. Globisch, M. Wiese, *J. Med. Chem.* **2004**, *47*, 2523–2533.
- [30] F. Tang, H. Ouyang, J. Z. Yang, R. T. Borchardt, *J. Pharm. Sci.* **2004**, *93*, 1185–1194.
- [31] G. F. Ecker, T. Stockner, P. Chiba, *Drug Discovery Today* **2008**, *13*, 311–317.
- [32] P. Chiba, M. Hitzler, E. Richter, M. Huber, C. Tmej, E. Giovagnoni, G. Ecker, *Quant. Struct.-Act. Relat.* **1997**, *16*, 361–366.
- [33] A. Seelig, E. Landwojtowicz, *Eur. J. Pharm. Sci.* **2000**, *12*, 31–40.
- [34] M. F. Rosenberg, G. Velarde, R. C. Ford, C. Martin, G. Berridge, I. D. Kerr, R. Callaghan, A. Schmidlin, C. Wooding, K. J. Linton, C. F. Higgins, *EMBO J.* **2001**, *20*, 5615–5625.
- [35] T. W. Loo, D. M. Clarke, *Biochem. Biophys. Res. Commun.* **2005**, *329*, 419–422.
- [36] S. G. Aller, J. Yu, A. Ward, Y. Weng, S. Chittaboina, R. Zhuo, P. M. Harrell, Y. T. Trinh, Q. Zhang, I. L. Urbatsch, G. Chang, *Science* **2009**, *323*, 1718–1722.
- [37] C. F. Higgins, *Nature* **2007**, *446*, 749–757.
- [38] Q. Qu, F. J. Sharom, *Biochemistry* **2002**, *41*, 4744–4752.
- [39] M. R. Lugo, F. J. Sharom, *Biochemistry* **2005**, *44*, 643–655.
- [40] T. W. Loo, D. M. Clarke, *J. Biol. Chem.* **2002**, *277*, 44332–44338.
- [41] J. W. Polli, S. A. Wring, J. E. Humphreys, L. Huang, J. B. Morgan, L. O. Webster, C. S. Serabjit-Singh, *J. Pharmacol. Exp. Ther.* **2001**, *299*, 620–628.
- [42] T. W. Loo, M. C. Bartlett, D. M. Clarke, *J. Biol. Chem.* **2003**, *278*, 1575–1578.
- [43] A. B. Shapiro, V. Ling, *J. Biol. Chem.* **1994**, *269*, 3745–3754.
- [44] M. Al-Shawi, A. E. Senior, *J. Biol. Chem.* **1993**, *268*, 4197–4206.
- [45] H. Yale, J. A. Bristol, *J. Heterocycl. Chem.* **1978**, *15*, 505–507.
- [46] A. F. Pozharskii, V. V. Kuz'menko, A. M. Simonov, *Khimiya Geterotsiklicheskikh Soedinenii* **1971**, *7*, 1105–1111.
- [47] K. Lewis, G. Casadei, *U.S. Pat. Appl. Publ.* **2008**, US 2008027044 A1.
- [48] G. A. Holloway, J. B. Baell, A. H. Fairlamb, P. M. Novello, J. P. Parisot, J. Richardson, K. G. Watson, *Bioorg. Med. Chem. Lett.* **2007**, *17*, 1422–1427.
- [49] V. A. Anisimova, M. V. Levchenko, A. F. Pozharski, *Khimiya Geterotsiklicheskikh Soedinenii* **1986**, *7*, 918–925.
- [50] V. A. Anisimova, T. B. Korochina, L. I. Zhurkina, *Khimiya Geterotsiklicheskikh Soedinenii* **1987**, *11*, 1496–1502.
- [51] V. A. Anisimova, A. M. Simonov, *Khimiya Geterotsiklicheskikh Soedinenii* **1975**, *2*, 258–262.
- [52] S. Suzuki, M. Kotake, M. Miyamoto, T. Kawahara, A. Kajiwara, I. Hishinuma, K. Okano, S. Miyazawa, R. Clark, F. Ozaki, N. Sato, M. Shinoda, A. Kamada, I. Tsukada, F. Matsuura, Y. Naoe, T. Terauchi, Y. Oohashi, O. Ito, H. Tanaka, et al., *PCT Int. Appl.* **2002**, WO 2002088094 A1.
- [53] N. Pietrancosta, A. Moumen, R. Dono, P. Lingor, V. Planchamp, F. Lamballe, M. Bähr, J. Kraus, F. Maina, *J. Med. Chem.* **2006**, *49*, 3645–3652.
- [54] M. Roe, A. Folkers, P. Ashworth, J. Brumwell, L. Chima, S. Hunjan, I. Pretswell, W. Dangerfield, H. Ryder, P. Charlton, *Bioorg. Med. Chem. Lett.* **1999**, *9*, 595–600.
- [55] G. L. Peterson, *Anal. Biochem.* **1977**, *83*, 346–356.
- [56] H. Müller, M. U. Kassack, M. Wiese, *J. Biomol. Screening* **2004**, *9*, 506–515.
- [57] R. A. Figler, H. Omote, R. K. Nakamoto, M. K. Al-Shawi, *Arch. Biochem. Biophys.* **2000**, *376*, 34–46.

Received: July 14, 2009

Revised: August 22, 2009

Published online on September 23, 2009